TAMPEREEN TEKNILLINEN YLIOPISTO
TAMPERE UNIVERSITY OF TECHNOLOGY

JOSE ENRIQUE VILLA ESCUSOL

COMPUTER SIMULATION AND MODELLING FOR INTELLIGENT CONTROL SYSTEMS IN SMALL FORESTRY MACHINES

Master of Science thesis

Examiner: Prof. Kari T. Koskinen
Examiner and topic approved by the Faculty Council of the Faculty of Engineering Science
on 8th June 2016

ABSTRACT

JOSE ENRIQUE VILLA ESCUSOL: Computer simulation and modelling for intelligent control systems in small forestry machines
Tampere University of Technology
Master of Science thesis, 51 pages, 7 Appendix pages
August 2016
Degree programme: Erasmus Exchange Student
Master's Degree in Industrial Engineering
Examiner: Prof. Kari T. Koskinen
Keywords: Forestry machine, modelling, control, simulation, Simulink, AMESim

In the forest industry, machines are equipped with robust and efficient hydraulic technology. However, the work profit depends heavily on the working operations with these machines. As a consequence, intelligent control systems are essential in these machines to try to improve work efficiency and variation between different human operators.

The main objective of this Master's Thesis is to obtain a linear trajectory control of a forestry crane in a miniature forest machine. To do that, it is important to study the system modeling using appropriate assumptions obtaining the most accurate response through the correct controller design. Moreover, simulation of the system using advanced modeling and simulation tool is run once that modeling has been done. This simulation has to include non-linearities of the components to obtain the most realistic results. To do that, MATLAB tools are used in modeling, control design and LMS Imagine.Lab AMESim is used in the final simulation. Control system is designed as Proportional Integral controller due to the fact that it is a simple controller for implementation.

This thesis is divided in two parts. First, in the theoretical chapter, modeling of the machine is obtained according to dynamics and kinematics of the forestry crane. In the second part, simulation in AMESim software is run to observe how the machine responds to an input signal according to the forestry crane trajectory.

PREFACE

This Master's Thesis is included as part of the cooperation between Usewood and Tampere University of Technology and it has been done in the department of Mechanical Engineering and Industrial Systems of Tampere University of Technology.

First of all, I want to thank my supervisors Jussi Aaltonen and Kari Koskinen for giving me the opportunity to do this Master's Thesis as an exchange student and for their guidance, help and ideas through the process of making this thesis. Moreover, I want to thank Olli Usenius and Usewood Forest Tec Oy for being all the time available for any help related to the forestry machine and the project.

Finally, I would like to express my gratitude to all the people that I met in these years of study, from the University of Zaragoza and Tampere University of Technology, and specially my family for supporting and encouraging me at every moment.

Tampere, 11.07.2016

Jose Enrique Villa Escusol

TABLE OF CONTENTS

LIST OF FIGURES

LIST OF TABLES

LIST OF ABBREVIATIONS AND SYMBOLS

TUT	Tampere University of Technology
DH	Denavit-Hartenberg
SI system	International System of Units
URL	Uniform Resource Locator
2D	Two-dimensional space
3D	Three-dimensional space
PI	Proportional Integral
PID	Proportional Integral Derivative
LS	Load-sensing
C-R	Compressibility + friction hydraulic line

a_i	Link length (DH notation) $[m]$
A	Orifice area $[m^2]$
$areap$	Equivalent orifice area in AMESim $[m^2]$
B_p	viscous damping coefficient of piston and load $[N/(m/s)]$
$C(q, \dot{q})$	Vector of Coriolis and centrifugal torques
C_{ep}	External leakage coefficient of piston
C_{ip}	Internal leakage coefficient of piston
C_d	Discharge coefficient
d_i	Link offset (DH notation) $[m]$
$D(q)$	Inertia matrix
dc_i	Hydraulic cylinder displacement $[m]$
dx	Differential of hydraulic cylinder displacement $[m]$
dq	Differential of hydraulic cylinder displacement $[rad]$
d_{spool}	Spool diameter $[m]$
d_p	Piston diameter $[m]$
d_r	Rod diameter $[m]$
$e(t)$	Error signal of the control system
F	Force produced by the cylinder $[N]$
F_{cyl}	Force generated or developed by piston
F_L	Arbitrary load force on piston
g	Gravity acceleration $[m/s^2]$
$g(q)$	Gravity torque vector

I_i	Moment of inertia of link i $[m^4]$
$J(q)$	Jacobian matrix
K	Kinetic energy function
K_s	Load spring gradient
K_p	Proportional gain
K_i	Integral gain
K_i	Derivative gain
L	Lagrangian function
L_{ci}	Length to the center of mass of link i $[m]$
L_i	Length of the link i $[m]$
l_i	Lengths link geometry $[m]$
m_i	Mass of the link i $[kg]$
M_t	Total mass of piston and load referred to piston $[kg]$
P	Potential energy function
P_s	Source pressure $[bar]$
P_t	Tank pressure $[bar]$
P_A	Pressure in the orifice A $[bar]$
P_B	Pressure in the orifice B $[bar]$
ΔP	Pressure drop across the orifice $[bar]$
q_1	Slewing joint angle $[rad]$
q_2	Inner boom joint angle $[rad]$
q_3	Outer boom joint angle $[rad]$
$\dot{q}_i$	Angular joint velocity of the link i $[rad/s]$
Q_A	Flow through orifice A $[m^3/s]$
Q_B	Flow through orifice B $[m^3/s]$
Q_a	Flow rate at port A in AMESim $[m^3/s]$
Q_t	Flow rate at port T in AMESim $[m^3/s]$
r_{ci}	Vector of coordinates of the i-link center of mass $[m]$
r_G	Radius of thin solid disk $[m]$
Rot	Rotational matrix
T	Homogeneous transformation
T_s	Sampling time $[s]$
$Trans$	Translational matrix
$u(t)$	output signal of the controller
v	Linear velocity $[m/s]$
V_0	Volume of chamber at initial moment $[m^3]$
V_1	Volume of forward chamber $[m^3]$

V_2	Volume of return chamber $[m^3]$
V_{i0}	Dead volume in the hydraulic cylinder $[m^3]$
x_v	Internal spool's displacement $[m]$
x_p	Actuator piston displacement $[m]$
$\dot{x}_p$	Actuator piston velocity $[m/s]$
X_{ref}	Forestry crane reference x-coordinate $[m]$
$X_{grapple}$	Forestry crane grapple x-coordinate $[m]$
Y_{ref}	Forestry crane reference y-coordinate $[m]$
$Y_{grapple}$	Forestry crane grapple y-coordinate $[m]$
α_i	Link twist (DH notation) $[rad]$
β	Angle for plane geometry $[rad]$
β_e	Bulk modulus $[bar]$
β_i	Fixed angles link geometry $[rad]$
γ_i	Variable angles link geometry $[rad]$
ω	Area gradient $[m]$
ω_n	Valve natural frequency $[s^{-1}]$
ψ	Angle for plane geometry $[rad]$
ρ	Density of the fluid $[kg/m^3]$
θ_i	Joint angle (DH notation) $[rad]$
τ	Torque applied to the body $[Nm]$
ξ	Valve damping ratio

1. INTRODUCTION

Forestry is an important field of industry. In 2015, according to official statistics released in March, forest industry was Finland's largest export sector. These exports were boosted by demand for pulp and paperboard.

In the forest industry, machines are equipped with robust and efficient hydraulic technology. However, the work profit depends heavily on the working operations with these machines. As a consequence, modern control systems are essential in these machines to try to reduce the human interaction in this industry. By using an autonomous control in the hydraulic system, it is possible to obtain a desired trajectory, which helps the driver to obtain the final position of the forestry crane.

This Master's Thesis has been conducted as part of the cooperation between Tampere University of Technology (TUT) and Usewood Forest Tec Oy, a Finnish company which provides machines and new methods to forest management.

The main purpose of this thesis is obtaining a modern control system, which will be able to help the driver in the cutting actions. Due to the fact that having a desired trajectory of the cutter ensures that working time is reduced, working efficiency is highly increased. Moreover, using this autonomous control, human interaction is not an element to consider.

Firstly, literary sources have been examined in order to obtain a general overview about what other researchers are doing about this topic ([3], [7], [6], [4], [5], [7], [17]). In order to obtain the simplest implementation of the control, linear control systems have been studied to design the correct controller. This part has been done using linear models of all parts of the forestry crane. After that, a simulation model of the crane is built and used to test the trajectory of the cutter body. The results of these simulation runs are discussed. Finally, possible future lines and conclusions are discussed.

2. MINIATURE FORESTRY MACHINES

Usewood Pro small harvester is designed for professional use as a working machine in the management of sapling stands. This machine has a power for young forest management due to the fact that is one of the smallest forest machines in the market. Due to small forest machine dimensions, the movement of the crane has to be really accurate to obtain really good results.

Figure 2.1 *Usewood Forest Master [19]*

2.1 The main working principle

This forestry machine is a type of an articulated manipulator with three revolute joints. This articulated manipulator is also called a revolute or anthropomorphic manipulator. It is a manipulator with three-joint structures which uses rotary joints

(q_1, q_2 and q_3) to access its work space. In this case, z_2 is parallel to z_1 and both z_1 and z_2 are perpendicular to z_0. Articulated manipulator structure and work space are shown in Figures 2.2 and 2.3. This configuration allows the gripper to reach a

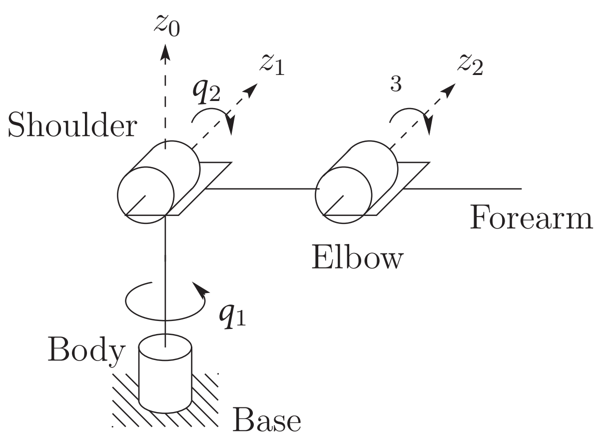

***Figure* 2.2** *Structure of the articulated manipulator (RRR) [15]*

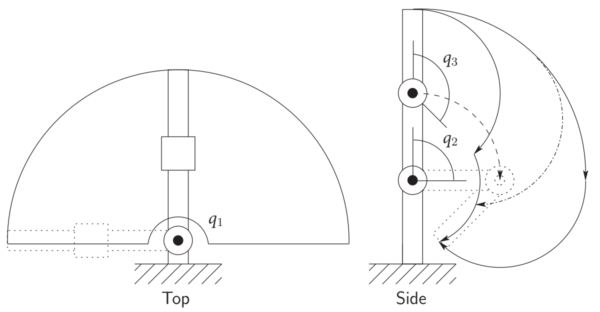

***Figure* 2.3** *Work space of the articulated manipulator (RRR) [15]*

wide working area. Moreover, in robotic systems, accuracy (attribute of how close the end-effector can come to a desired point) and repeatability (attribute of how close the end-effector can return to a previously taught point) are highly dependent on the joints, control and working components.

To reach a given point with accuracy and repeatability, the intelligent control system has to vary the joint angles correctly. These joint angles are moved using hydraulic cylinders, which increasing or decreasing its piston displacement creates a torque, which is able to move the forestry crane.

The hydraulic system used in this mobile application is the Load-Sensing control, which is shown in Figure 2.4. This system is used in forest machines or excavators among others due to the fact that high flow is needed and load pressure varies remarkably. The load pressure is controlled by the Load sensing system. This load pressure sets the supply pressure and pump flow rate according to the operation point. An important characteristic is that independent movement during parallel operation is allowed.

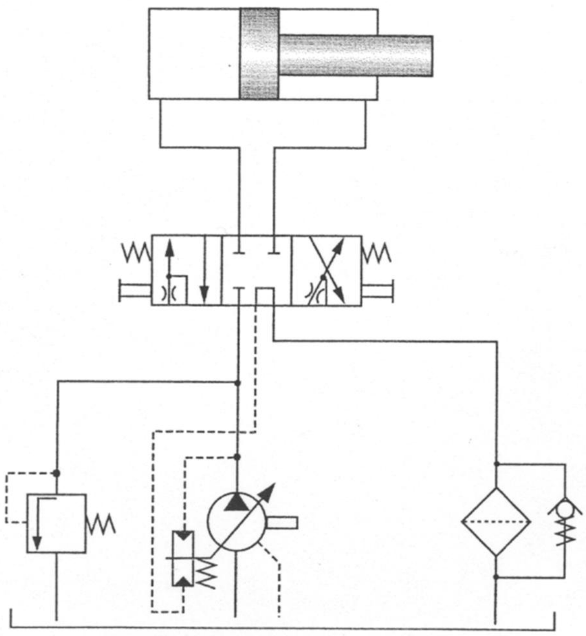

Figure 2.4 *Load-Sensing control made by variable hydraulic pump [13]*

The spool displacement of the proportional valve, which varies the flows through this component, is controlled using the intelligent control system. This control system is responsible for obtaining the input signal required to achieve the desired joint angle in the forestry crane.

2.2 Introduction of the problem

Human operators in forestry machines have to manage lots of different actions at the same time while they are driving or working. It means that there are several tasks performed at the same time such as maneuvering of the vehicle, controlling the crane actuators and cutting operations. As a consequence, the drivers experience and skills are essential if there is not any automatic control in the machine. However, if control systems are included, these skills are not really important to obtain good results and everyone is able to do this job as a professional driver.

The concept of designing autonomous operations for this industry has been continuing from the 1980s. The state-of-the-art in crane control consists of using dual analog joysticks which provide electrical signals that command the flow rate of the hydraulic system, which is formed by a proportional valve and a hydraulic cylinder. These valves control each hydraulic actuator and each boom joint independently.

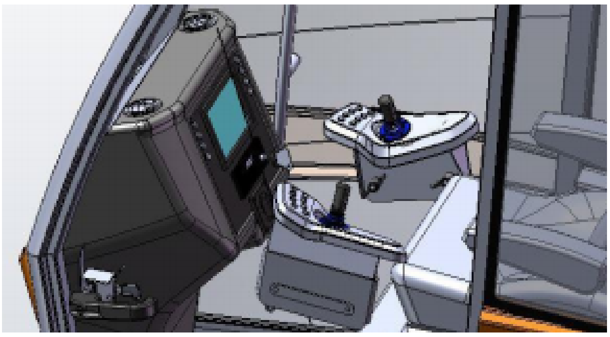

Figure 2.5 *Usewood cabin with ergonomic joystick [20]*

Due to the fact that the boom joints and the joysticks are moving independently, the driver's skills are essential in obtaining an efficient work. Using modern control systems instead of joysticks in the cutting operations can be useful to get easier boom operations which help the forestry driver daily.

2.3 Purpose and objectives

The main purpose of this Master's Thesis is the obtaining of a simple controller, which is able to control the boom operations, having a linear trajectory of the forestry crane. Due to this trajectory, it will be possible to get the desired movement through the working place without any human interaction.

In Figure 2.6, the three joints of the forestry crane are shown: slewing q_1, inner boom q_2 and outer boom q_3. Moreover, it is possible to see the two essential reference axis of the machine where the grapple is defined as the point where the cutter is positioned.

First of all, system modeling is done using appropriate assumptions to obtain the

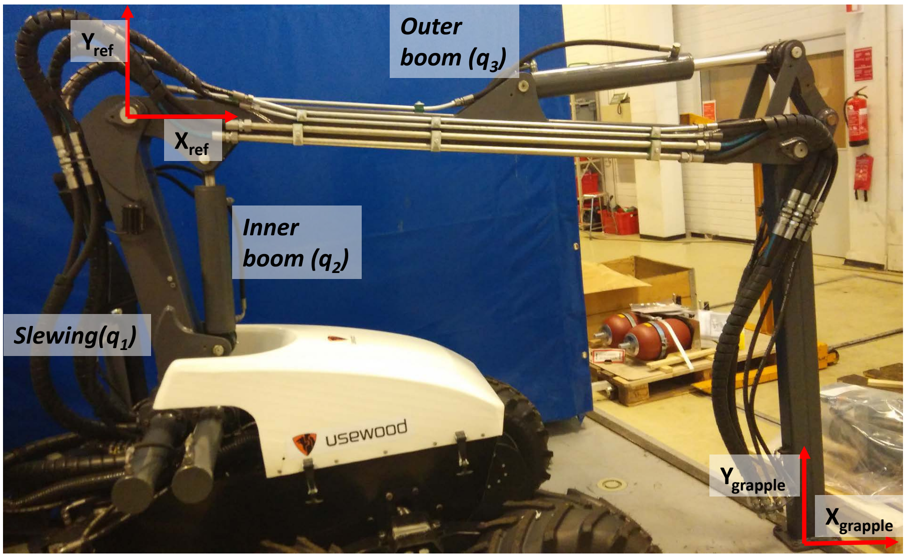

Figure 2.6 *Real Usewood machine from the laboratory*

most accurate response and to design the correct linear controller. This linear controller is designed as a Proportional-Integral controller (PI controller). It is used to simplify the implementation in the real machine. To do that, MATLAB and Simulink are used to facilitate the obtaining of mathematical expressions, getting the performance and the simulation of the ideal and linear control system.

The system modeling is done in the following two parts: kinematics and dynamics. The relation between the joint angles q_2 and q_3 and the final grapple point $[X_{grapple}, X_{grapple}]$ is described in the kinematic section. After that, mechanical dynamics is studied to obtain the relation between the forestry crane bodies and the torque in the joints. Hydraulic dynamics explains how this torque varias as a function of the input signal in the hydraulic system.

Once the modelling and design of the controller have been done, the complete simulation of the forestry crane is done using LMS Imagine.Lab AMESim. Using this advanced simulation tool, it is possible to include non-linearities in the hydraulic and mechanical systems, which are difficult to model and include in the MATLAB control design.

3. SYSTEM MODELING

3.1 Forestry crane kinematics

Any robot or machine can be described kinematically by giving the values of four parameters for each link. These parameters are a convention called the Denavit-Hartenberg notation [2]. Two of these parameters describe the link itself and the others describe the connection between the link and its neighbour. In the case of this machine, all joints are revolute, θ_i is called the joint variable and the other three would be fixed link parameters.

These parameters and reference frames of the forestry crane can be seen in 3.1

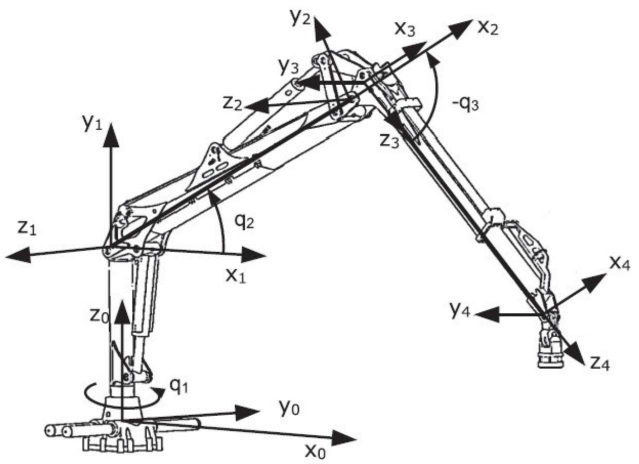

Figure 3.1 *Reference frames to specify the DH convention (adapted from [12])*

The main objective of this study is to obtain a linear movement of the forestry crane cutter. It means that the machine will be moved in 2D instead of 3D. As a consequence, to have a simple forest machine system, the Denavit-Hartenberg parameters will be obtained only in 2D. Due to that simplification, z-axis will be fixed around the system so link 1 will be fixed too (no movement around z_0 axis). According to the definition of these parameters, the values for each joint in the forestry crane can be defined by:

Link i	θ_i	d_i (m)	a_i (m)	α_i (rad)
1	q_2	0	0	0
2	q_3	0	L_2	0
3	0	0	L_3	0

Table 3.1 *DH parameters of the two-link manipulator*

Using Denavit-Hartenberg parameters, the forestry crane can be defined by joint angles θ, link offset d, link length a and link twist α. The model and simulation in software will be done following these characteristics of the system and doing some simplifications about the movement and components which will be described below.

3.2 Geometric direct model

The purpose of this Master's Thesis is the control of the linear trajectory of the forestry crane. This linear trajectory is defined by Cartesian coordinate system. As a requirement, it is necessary to obtain the relation between this coordinate system and the joints angles of the forestry crane. This relation is calculated based on the geometric solution of a simple planar two-link manipulator.

To find a manipulator's joint angles solution in a geometric method, it is necessary to decompose the spatial geometry of the arm into several plane-geometry problems. These joint angles can be solved using trigonometric relations applying directly plane geometry.

Figure 3.2 shows the triangle formed by L_2, L_3 and the line joining the origin of frame 1 with the origin of frame 3. Two different configurations can be seen in this figure, elbow-up and elbow-down (dashed lines). Both of them are related to the position of the forest machine arms. In the case of study, elbow-up configuration will be used. Considering the solid triangle (elbow-up) and applying the law of cosines to solve θ_3, it is possible to obtain this joint angle depending on x and y coordinates.

$$q_3 = \arccos\left(\frac{\mathrm{L_2}^2 + \mathrm{L_3}^2 - x^2 - y^2}{2\,\mathrm{L_2}\,\mathrm{L_3}}\right) - \pi, \tag{3.1}$$

In order to confirm this solid triangle, one working condition has to be declare. This

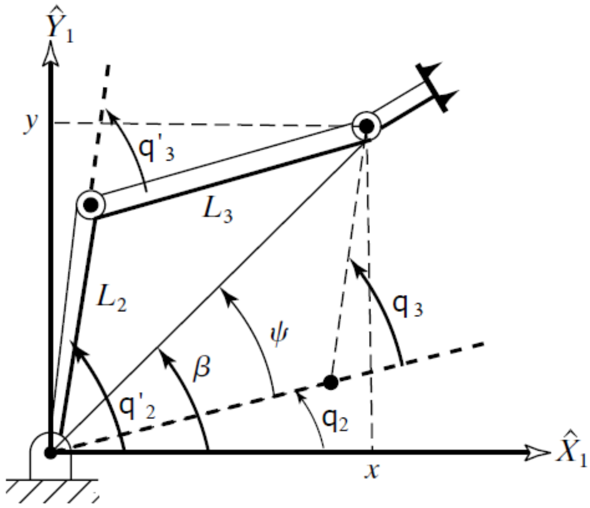

Figure 3.2 *Plane geometry of the manipulator (adapted from [1])*

condition would be checked at this point in an algorithm to verify the existence of solutions for the forestry crane.

$$\sqrt{x^2 + y^2} \leq \mathrm{L}_2 + \mathrm{L}_3 \tag{3.2}$$

Following DH-Parameters and using the angle definition of the figure 3.2, different machine configurations depend on the sign of q_3:

- Elbow-up (solid triangle): if q_3 lower than 0 then $q_2 = \beta + \psi$
- Elbow-down (dashed-line triangle): if q_3 higher than 0 then $q_2 = \beta$ - ψ

To solve q_2, expressions for angles β and ψ have to be defined. Firstly, β may be in any quadrant depending on the signs of x and y. This angle can be obtained using two-argument arctangent:

$$\beta = \arctan(x, y) \tag{3.3}$$

To find ψ, law of cosines has to be used again:

$$\psi = \arccos\left(\frac{\sqrt{x^2 + y^2}}{2\,\mathrm{L}_2}\right) \tag{3.4}$$

Finally, using elbow-down configuration for the forestry crane, the joint angle θ_2 is:

$$q_2 = \arctan\left(\frac{x}{y}\right) + \arccos\left(\frac{\sqrt{x^2+y^2}}{2\,\mathrm{L}_2}\right) \tag{3.5}$$

3.3 Inverse manipulator kinematics

The system will be simplified to a planar elbow manipulator with two revolute joints.

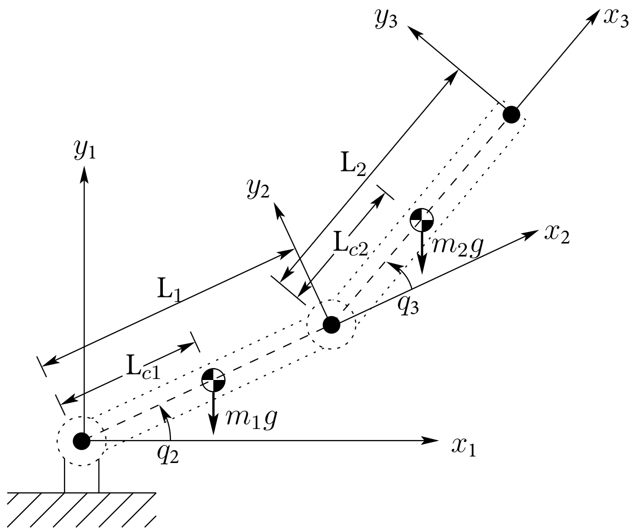

Figure 3.3 *Two link revolute joint arm (adapted from [15])*

In the Figure 3.3, for i = 2,3, q_i denotes the joint angle, m_i denotes the mass of link i, L_i denotes the length of the link i, L_{ci} denotes the distance from the previous joint to the center of mass of link i, and I_i denotes the moment of inertia of link i about the axis coming out of the page.

This part of the modelling is important to obtain the mechanical dynamics of the forestry crane due to the fact that Jacobian matrices of mass points and final joints are necessary. These are calculated based on algebraic solution of inverse manipulator kinematics. In the field of robotics, Jacobians are generally used relating joint velocities to Cartesian velocities of the tip of the arm. As a requirement, linear velocities have to be calculated to get these Jacobian matrices.

$$v = J(q)\dot{q} \tag{3.6}$$

Firstly, transformation matrices for each link have to be defined. A commonly used convention for selecting frames of reference in robotic applications is the DH convention. Using the parameters described above, each homogeneous transformation T_i is obtained as a product of four basic transformations, where the four variables θ, a, d and α are DH parameters [15].

$$T_i = Rot_{z,\theta_i} Trans_{z,d_i} Trans_{x,a_i} Rot_{x,\alpha_i} = \\ = \begin{pmatrix} cos\theta_i & -sin\theta_i cos\alpha_i & sin\theta_i sin\alpha_i & a_i cos\theta_i \\ sin\theta_i & cos\theta_i cos\alpha_i & -cos\theta_i sin\alpha_i & a_i sin\theta_i \\ 0 & sin\alpha_i & cos\alpha_i & d_i \\ 0 & 0 & 0 & 1 \end{pmatrix} \tag{3.7}$$

Once those link frames have been defined and the link parameters found, link transformations can be multiplied to find the single transformation that relates frame N to frame 0.

$$^{0}_{N}T = {}^{0}_{1}T\, {}^{1}_{2}T\, {}^{2}_{3}T \, ... \, {}^{N-1}_{N}T \tag{3.8}$$

Doing a simplify of Table 3.1, it is possible to obtain the DH parameters of the link-arm manipulator from Figure 3.3

Link i	θ_i	d_i (m)	a_i (m)	α_i (rad)
1	q_2	0	L_2	0
2	q_3	0	L_3	0

Table 3.2 *DH parameters of the two-link manipulator after simplification*

Using the concatenating link transformations and having the frame 1 as a reference,forestry crane link transformations are:

$$^{2}_{1}T = \begin{pmatrix} \cos(\mathrm{q}_2) & -\sin(\mathrm{q}_2) & 0 & \mathrm{L}_2\cos(\mathrm{q}_2) \\ \sin(\mathrm{q}_2) & \cos(\mathrm{q}_2) & 0 & \mathrm{L}_2\sin(\mathrm{q}_2) \\ 0 & 0 & 1 & 0 \\ 0 & 0 & 0 & 1 \end{pmatrix}, \tag{3.9}$$

$$^{3}_{1}T = \begin{pmatrix} \cos(\mathrm{q}_2+\mathrm{q}_3) & -\sin(\mathrm{q}_2+\mathrm{q}_3) & 0 & \mathrm{L}_3\cos(\mathrm{q}_2+\mathrm{q}_3)+\mathrm{L}_2\cos(\mathrm{q}_2) \\ \sin(\mathrm{q}_2+\mathrm{q}_3) & \cos(\mathrm{q}_2+\mathrm{q}_3) & 0 & \mathrm{L}_3\sin(\mathrm{q}_2+\mathrm{q}_3)+\mathrm{L}_2\sin(\mathrm{q}_2) \\ 0 & 0 & 1 & 0 \\ 0 & 0 & 0 & 1 \end{pmatrix}, \tag{3.10}$$

After that, Cartesian velocities can be defined using these link transformations.

Following Craig notation [1], the linear velocity of the frame's origin is the same as frame's origin i plus a new component caused by rotational velocity of link i. (See Equation 3.11 where P is the constant distance between two frames).

$$ {}^{i}v_{i+1} = {}^{i}v_{i} + {}^{i}\dot{q}_{i+1} \times {}^{i}P_{i+1} \tag{3.11}$$

The final linear velocity is defined multiplying both sides by R:

$$ {}^{i+1}v_{i+1} = {}^{i+1}_{i}R({}^{i}v_{i} + {}^{i}\dot{q}_{i+1} \times {}^{i}P_{i+1}) \tag{3.12}$$

Using the previous equation, mass points and final joint linear velocities are defined as follows.

$$ v_{c2} = \begin{pmatrix} -\mathrm{L_{c2}}\sin(\mathrm{q_2})\,\dot{q_2} \\ \mathrm{L_{c2}}\cos(\mathrm{q_2})\,\dot{q_2} \\ 0 \end{pmatrix} \tag{3.13}$$

$$ v_{c3} = \begin{pmatrix} -\mathrm{L_{c3}}\sin(\mathrm{q_2}+\mathrm{q_3})\,(\dot{q_2}+\dot{q_3}) - \mathrm{L_2}\sin(\mathrm{q_2})\,\dot{q_2} \\ \mathrm{L_{c3}}\cos(\mathrm{q_2}+\mathrm{q_3})\,(\dot{q_2}+\dot{q_3}) + \mathrm{L_2}\cos(\mathrm{q_2})\,\dot{q_2} \\ 0 \end{pmatrix} \tag{3.14}$$

$$ v_{3} = \begin{pmatrix} -\mathrm{L_{3}}\sin(\mathrm{q_2}+\mathrm{q_3})\,(\dot{q_2}+\dot{q_3}) - \mathrm{L_2}\sin(\mathrm{q_2})\,\dot{q_2} \\ \mathrm{L_{3}}\cos(\mathrm{q_2}+\mathrm{q_3})\,(\dot{q_2}+\dot{q_3}) + \mathrm{L_2}\cos(\mathrm{q_2})\,\dot{q_2} \\ 0 \end{pmatrix} \tag{3.15}$$

Finally, once that linear velocities have been calculated, Jacobian matrices are obtained. The Jacobian is a multidimensional form of the derivative.

$$ J(v,\theta) = \frac{\partial v}{\partial \theta} = \begin{bmatrix} \frac{\partial v_x}{\partial \theta_2} & \frac{\partial v_x}{\partial \theta_3} \\ \frac{\partial v_y}{\partial \theta_2} & \frac{\partial v_y}{\partial \theta_3} \end{bmatrix} \tag{3.16}$$

As a consequence, Jacobians for each linear velocity are:

$$ J_{vc2} = \begin{pmatrix} -\mathrm{L_{c2}}\sin(\mathrm{q_2}) & 0 \\ \mathrm{L_{c2}}\cos(\mathrm{q_2}) & 0 \\ 0 & 0 \end{pmatrix} \tag{3.17}$$

$$J_{vc3} = \begin{pmatrix} -\mathrm{L}_{c3}\ \sin(\mathrm{q}_2 + \mathrm{q}_3) - \mathrm{L}_2\ \sin(\mathrm{q}_2) & -\mathrm{L}_{c3}\ \sin(\mathrm{q}_2 + \mathrm{q}_3) \\ \mathrm{L}_{c3}\ \cos(\mathrm{q}2 + \mathrm{q}_3) + \mathrm{L}_2\ \cos(\mathrm{q}_2) & \mathrm{L}_{c3}\ \cos(\mathrm{q}_2 + \mathrm{q}_3) \\ 0 & 0 \end{pmatrix} \tag{3.18}$$

$$J_{v3} = \begin{pmatrix} -\mathrm{L}_3\ \sin(\mathrm{q}_2 + \mathrm{q}_3) - \mathrm{L}_2\ \sin(\mathrm{q}_2) & -\mathrm{L}_3\ \sin(\mathrm{q}_2 + \mathrm{q}_3) \\ \mathrm{L}_3\ \cos(\mathrm{q}2 + \mathrm{q}_3) + \mathrm{L}_2\ \cos(\mathrm{q}_2) & \mathrm{L}_3\ \cos(\mathrm{q}_2 + \mathrm{q}_3) \\ 0 & 0 \end{pmatrix} \tag{3.19}$$

3.4 Mechanical dynamics

In control and robotics, two of the methods most used for mechanical systems are Euler-Lagrange and Hamiltonian equations. In this case, Euler-Lagrange equations have been used to describe the mechanical dynamics of the forestry crane. These equations describe the time evolution of mechanical systems subjected to holonomic constraints, when the constraint forces satisfy the principle of virtual work.

If the Lagrangian function L of the system is defined as the difference of the kinetic and potential energy (Equation 3.20), it is possible to obtain the Euler-Lagrange equation as Equation 3.21. These equations provide a formulation of the dynamic equations of motion equivalent to those derived using Newton's Second Law [15].

$$L = K - P \tag{3.20}$$

$$\frac{d}{dt}\frac{\partial L}{\partial \dot{y}} - \frac{\partial L}{\partial y} = f \tag{3.21}$$

It is common to write the Euler-Lagrange equations as a matrix form (Equation 3.22). This matrix form relates the derivatives of joint variables with the Lagrangian parameters where $D(q)$ is the inertia matrix, $C(q, \dot{q})$ is the vector of Coriolis and centrifugal torques and $g(q)$ is the gravity torque vector. The sum of these variables equals torque τ applied to the body.

$$D(q)\ddot{q} + C(q, \dot{q})\dot{q} + g(q) = \tau \tag{3.22}$$

Due to the fact that joint velocities are small while forestry crain is moving , it is possible to ignore $C(q, \dot{q})$ which contains second-order velocity terms [18]. Due to that assumption, Euler-Lagrange equations depend only on acceleration and position of the joints.

$$D(q)\ddot{q} + g(q) = \tau \tag{3.23}$$

The kinetic energy of a rigid object, it is the sum of translational energy obtained by concentrating the entire mass of the object at the center of mass and the rotational kinetic energy of the body about the center of mass. Considering a n-link manipulator, linear and angular velocities can be expressed in terms of the Jacobian matrix and the derivative of the joint variables. As a consequence, the overall kinetic energy of the manipulator equals to Equation 3.24 or Equation 3.25 using inertia matrix $D(q)$.

$$K = \frac{1}{2}\dot{q}^T \sum_{i=1}^{n} [m_i J_{v_i}(q)^T J_{v_i}(q) + J_{\omega_i}(q)^T R_i(q) I_i R_i(q)^T J_{\omega_i}(q)]\dot{q} \tag{3.24}$$

$$K = \frac{1}{2}\dot{q}^T D(q)\dot{q} \tag{3.25}$$

In this case, translational part of the kinetic energy is

$$\frac{1}{2}m_1 v_{c1}^T v_{c1} + \frac{1}{2}m_1 v_{c2}^T v_{c2} + \frac{1}{2}m_1 v_2^T v_2 = \frac{1}{2}\dot{q}^T(m_1 J_{v_{c1}}^T J_{v_{c1}} + m_2 J_{v_{c2}}^T J_{v_{c2}} + m_G J_{v_2}^T J_{v_2})\dot{q} \tag{3.26}$$

Rotational kinetic energy of the overall system is based on the angular velocity terms. These terms expressed in the base of inertial frame are shown in Equation 3.27. Due to the fact that angular velocity is aligned with k (z-axis), rotational kinetic energy can be shown in Equation 3.28

$$\omega_1 = \dot{q}_1 k \qquad , \qquad \omega_2 = (\dot{q}_1 + \dot{q}_2)k, \tag{3.27}$$

$$\frac{1}{2}\dot{q}^T \left\{ I_1 \begin{bmatrix} 1 & 0 \\ 0 & 0 \end{bmatrix} + I_2 \begin{bmatrix} 1 & 1 \\ 1 & 1 \end{bmatrix} + I_G \begin{bmatrix} 1 & 1 \\ 1 & 1 \end{bmatrix} \right\} \dot{q}, \tag{3.28}$$

where moments of inertia I_i are defined in Equations 3.29, 3.30 and 3.31. I_2 and I_G are obtained as a rod of length L_i and mass m_i rotating about its center and I_G is obtained as a thin solid disk of radius r_G and mass m_G.

$$I_2 = \frac{1}{12} * m_2 * L_2^2 \tag{3.29}$$

$$I_3 = \frac{1}{12} * m_3 * L_2^3 \tag{3.30}$$

$$I_G = \frac{1}{2} * m_2 * r_G^2; \tag{3.31}$$

After obtaining translational and rotational kinetic energy based on the two-link revolute joint arm configuration and the previous equations, Inertia Matrix D(q) is

$$D(q) = \begin{pmatrix} m_G\, {L_3}^2 + L_2\, m_G\, \cos(q_3)\; L_3 + m_3\, {L_{c3}}^2 + \mathrm{L_2\, m_3\, \cos(q_3)\; L_{c3} + I_3 + I_G} \\ \mathrm{m_G\, {L_3}^2 + m_3\, {L_{c3}}^2 + I_3 + I_G} \end{pmatrix}, \tag{3.32}$$

After that, potential energy term has to be defined. In the case of rigid dynamics, the only source of potential energy is the gravity. The total potential energy of the n-link robot can be computed by assuming that the whole arm mass is located at its center of mass (Equation 3.33), where g is the vector giving the direction of gravity and vector r_{ci} gives the coordinates of the i-link center of mass.

$$P = \sum_{i=1}^{n} P_i = \sum_{i=1}^{n} g^T r_{ci} m_i, \tag{3.33}$$

According to the total potential energy, the functions $g(q_i)$ are defined as

$$g(q_i) = \frac{\partial P}{\partial q_i}, \tag{3.34}$$

To have a simplification of the mechanical torques in the modeling, hydraulic cylinders will be moved alternately. It means that second cylinder will be fixed while first cylinder is moving, and vice versa. In this assumption of the system, joint acceleration in the another cylinder of study will be zero, and the joint position will be fixed to obtain the necessary torque.

Finally, it is possible to write down the dynamical equations of the system as in Equation 3.23.

$$\begin{aligned} \tau_2 = \ddot{q}_2\, &[\mathrm{I_2 + I_3 + I_G + {l_2}^2\, m_3 + {l_2}^2\, m_G + {l_3}^2\, m_G + lc2^2\, m_2 + lc3^2\, m_3} \\ &+ \mathrm{2\, l_2\, l_3\, m_G\, \cos\,(q_3) + 2\, l_2\, l_{c3}\, m_3\, \cos\,(q_3)]} \\ &+ g\, \mathrm{m_G\, [l_3\, \cos\,(q_2 + q_3) + l_2\, \cos\,(q_2)]} \\ &+ g\, \mathrm{m_3\, [l_{c3}\, \cos\,(q2 + q_3) + l_2\, \cos\,(q_2)]} + g\, \mathrm{l_{c2}\, m_2\, \cos\,(q_2)}, \end{aligned} \tag{3.35}$$

$$\tau_3 = \ddot{q}_3\, \left(\mathrm{m_G\, {l_3}^2 + m_3\, {l_{c3}}^2 + I_3 + I_G}\right) + g\, \mathrm{l_3\, m_G\, \cos(q_2 + q_3)} + g\, \mathrm{l_{c3}\, m_3\, \cos(q_2 + q_3)}\,, \tag{3.36}$$

3.5 Joint torques and hydraulic forces

The previous section defines the joint torques according to kinetic and potential energy of the system. Once these torques have been obtained, the next step will be finding the relation with the hydraulic cylinder force.

The relation between hydraulic force and mechanical torque is defined by the principle of virtual work (Equation 3.37). This principle can be stated in words as the work done by external forces when any corresponding set of virtual displacement is zero. As a consequence, mechanical torque is defined in Equation 3.38.

$$\tau dq = F dx, \tag{3.37}$$

$$\tau = F\frac{dx}{dq}, \tag{3.38}$$

$$J(q) = \frac{dx}{dq}, \tag{3.39}$$

where F_i is the force produced by the cylinder and $J(q)$ denotes the change of the hydraulic cylinder displacement x with respect to the angular link position q. The derivative $J(q)$ (equation 3.39) is obtained using trigonometric mapping.

3.5.1 Finding the relation $\mathbf{dc_2(q_2)}$

In order to calculate the change of linear piston displacement dc_2 as a function of the measured joint angle q_2, trigonometric relations are used.

As it can be seen in Figure 3.4, the hydraulic cylinder displacement is defined by law of cosines, obtaining a function which relates body part dimensions and the first link joint.

$$dc_2 = \sqrt{\mathrm{l_1}^2 - 2\,\cos\left(\beta_1 - \frac{\pi}{2} + \beta_2 - \mathrm{q_2}\right)\,\mathrm{l_1}\,\mathrm{l_2} + \mathrm{l_2}^2}, \tag{3.40}$$

3.5.2 Finding the relation $\mathbf{dc_3(q_3)}$

In the same way as the previous relation, trigonometrical relations also define the change of dc_3 as a function of q_3. However, due to the fact that the second cylinder is connected to the second arm using a quadrangle, the relationship will be more

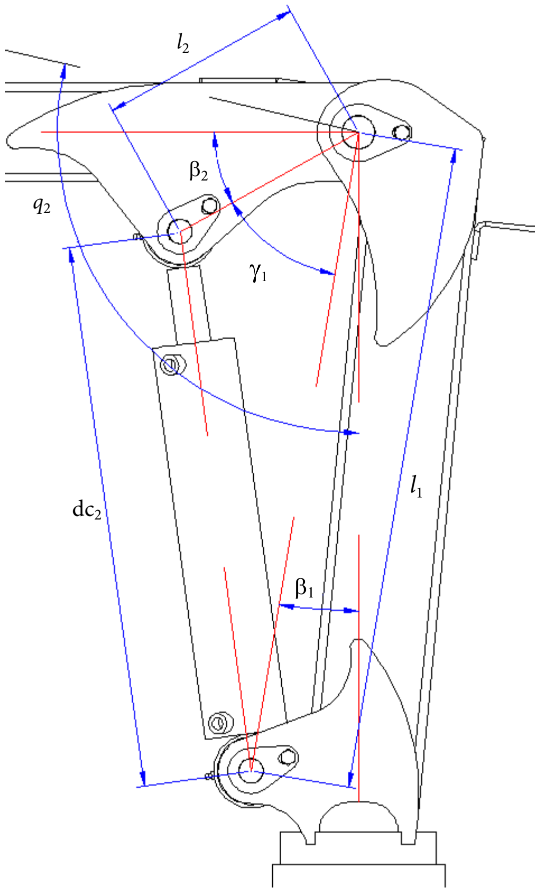

Figure 3.4 *First link geometry as function of the hydraulic cylinder*

complex. The schematic presented in Figure 3.5 allows defining the geometric relations.

In the second cylinder, the angle between l_3 and l_4 is related to joint link angle q_3 through γ_2, γ_3 and d_1.

$$\gamma_2 = \frac{\pi}{2} + \beta_3 - \beta_4 - \beta_5 - \mathrm{q}_3, \tag{3.41}$$

$$d_1 = \sqrt{\mathrm{l_3}^2 - 2\cos(\gamma_2)\,\mathrm{l}_3\,\mathrm{l}_4 + \mathrm{l_4}^2}, \tag{3.42}$$

$$\gamma_{34} = \arccos\left(\frac{\mathrm{d_1}^2 + \mathrm{l_3}^2 - \mathrm{l_4}^2}{2\,\mathrm{d}_1\,\mathrm{l}_3}\right) + \arccos\left(\frac{\mathrm{d_1}^2 + \mathrm{l_5}^2 - \mathrm{l_6}^2}{2\,\mathrm{d}_1\,\mathrm{l}_5}\right), \tag{3.43}$$

Once that γ_{34} has been defined, it is possible to obtain γ_5 by the angle differences

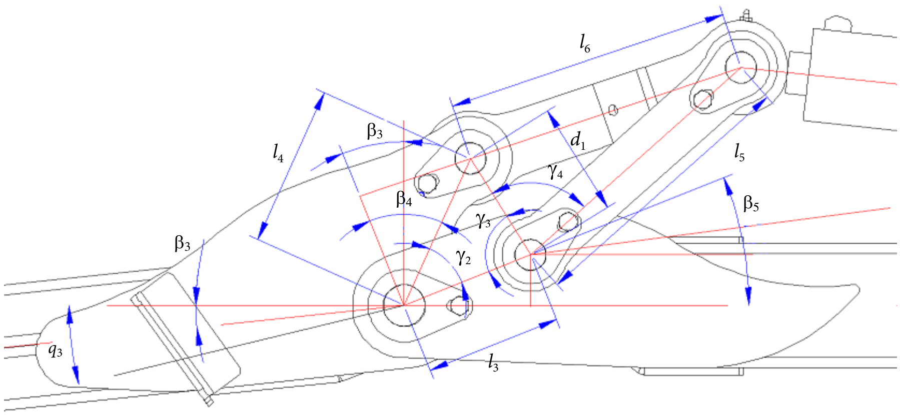

(a)

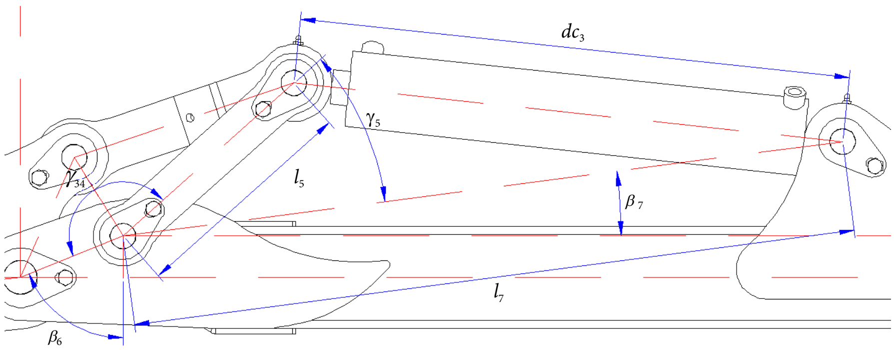

(b)

Figure 3.5 *Second link geometry as function of the hydraulic cylinder*

and afterwards dc_3 using law of cosines.

$$\gamma_5 = 2\pi - \frac{\pi}{2} - \beta_6 - \beta_7 - \gamma_{34}, \tag{3.44}$$

$$dc_3 = \sqrt{\mathrm{l_5}^2 - 2\,\cos(\gamma_5)\ \mathrm{l_5}\,\mathrm{l_7} + \mathrm{l_7}^2}, \tag{3.45}$$

After the definition of the hydraulic cylinder displacement with respect to the angular link position $dc_i(q_i)$, it is possible to obtain the derivative $J(q)$. Finally, using the previous equation 3.38 and the actuator displacement dc_i as x, the vector of generalized forces is

$$\tau = \begin{bmatrix} \frac{\partial dc_2}{\partial q_2}\ F_2 \\ \frac{\partial dc_3}{\partial q_3}\ F_3 \end{bmatrix} = \begin{bmatrix} J(q_2)\ F_2 \\ J(q_3)\ F_3 \end{bmatrix}, \tag{3.46}$$

3.6 Hydraulic component dynamics

A typical hydraulic system consists of a pump, one or more control valves and a hydraulic actuator. In this case of study, pump will be simplified as a constant flow source with a relief valve which controls the maximum pressure of the source line. Thus, only proportional valve and hydraulic cylinder dynamics are studied in the following sections.

3.6.1 Proportional valve

The proportional valve used to drive the oil in this system is a typical three-land-four-way spool valve (Figure 3.6). In this figure, pressures P_s and P_t correspond to the source and tank pressures respectively.

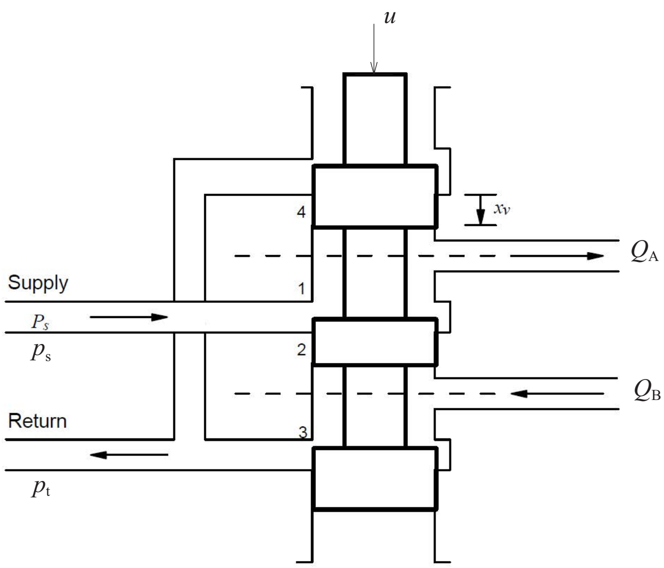

Figure 3.6 *Three-land-four-way spool valve (adapted from [8])*

This hydraulic component has orifices with variable areas controlled by the internal spool's displacement x_v. This displacement will be explained below. The flow through an orifice is given by the general equation [11]:

$$Q = C_d \, A \sqrt{\frac{2}{\rho} \, \Delta P}, \tag{3.47}$$

where C_d is called discharge coefficient which is approximately equal to the contraction coefficient, ΔP is the pressure drop across the orifice, ρ is the density of the fluid and A is the orifice area which depends on valve geometry.

In this case, it is assuming that valve orifices are matched and symmetrical, which is the case for most of the spool valves manufactured. As a consequence, only one orifice, i.e., orifice A, is needed to be defined in the proportional valve dynamic.

$$A_1(x_v) = A_3(x_v) = A_2(-x_v) = A_4(-x_v) = A(x_v), \tag{3.48}$$

Moreover, if the orifice areas are linear with valve stroke, only one parameter is required. This parameter is called area gradient w and it is related to the width of the slot in the valve sleeve. Area gradient is the rate of change of orifice area with stroke. The relationship between w and A is given by

$$A = w\, x_v, \tag{3.49}$$

where

$$w = \pi d_{spool}, \tag{3.50}$$

According to the modeling of the proportional valve flows, Equation 3.47 can be rewritten to obtain flows Q_A and Q_B, which go to and come from the hydraulic cylinder respectively.

$$Q_A = C_d\, w\, x_v \sqrt{\frac{2}{\rho}|\Delta P_A|}, \tag{3.51}$$

$$Q_B = C_d\, w\, x_v \sqrt{\frac{2}{\rho}|\Delta P_B|}, \tag{3.52}$$

where

$$\Delta P_A = \begin{cases} P_s - P_A & \text{if } x_v > 0 \\ P_A - P_t & \text{if } x_v < 0 \end{cases} \tag{3.53}$$

$$\Delta P_B = \begin{cases} P_B - P_t & \text{if } x_v > 0 \\ P_s - P_B & \text{if } x_v < 0 \end{cases} \tag{3.54}$$

As it can be seen in Equations 3.53 and 3.54, the response of the system differs according to the direction of motion in the proportional valve [5]. It means that the orifice flow changes in relation to the sign of the spool displacement. To place this considerations in mathematical terms, it is possible to consider from 3.51, 3.52, 3.53 and 3.54 that

$$Q_A = C_d\, w\, x_v \sqrt{\frac{2}{\rho}\left|\frac{P_s - P_t}{2} + sign(x_v)\left(\frac{P_s + P_t}{2} - P_A\right)\right|}, \tag{3.55}$$

$$Q_B = C_d\ w\ x_v \sqrt{\frac{2}{\rho} \left| \frac{P_s - P_t}{2} - sign(x_v) \left(\frac{P_s + P_t}{2} - P_B \right) \right|}, \tag{3.56}$$

According to spool valve displacement, its dynamics can be derived following a linear second order differential equation, which is a widely used with sufficient approximation [16].

$$\frac{d^2 x_v(t)}{dt^2} + 2\ \omega_n\ \xi\ \frac{dx_v(t)}{dt} + \omega_n^2 x_v(t) = \omega_n^2\ u(t), \tag{3.57}$$

Typical values of spool valve parameters are: natural frequency $\omega_n = 30 - 50Hz$ and damping ratio $\xi = 0.7 - 1.0$.

3.6.2 Hydraulic cylinder

Once the proportional valve flows have been defined as a function of the spool valve displacement, it is possible to obtain the relation between its input signal and the hydraulic cylinder displacement using hydraulic cylinder dynamics. As it was discussed earlier, proportional valve orifices are assumed to be matched and symmetrical. According to equation 3.58 (state equation) and 3.59 (continuity

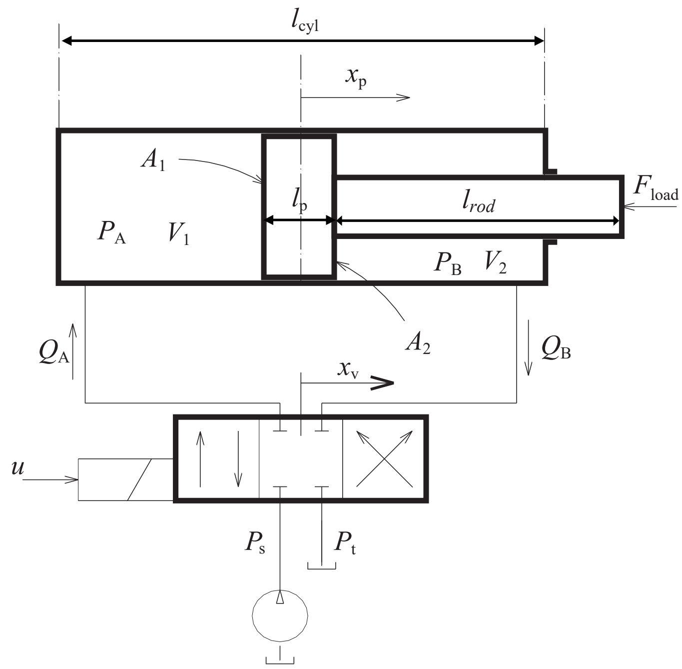

Figure 3.7 *Schematic diagram of a hydraulic actuator (adapted from [16])*

equation), it is possible to combine both to get a more useful one (Equation 3.60) [11].

$$\rho = \rho_i + \frac{\rho_i}{\beta_e} P, \tag{3.58}$$

$$\sum W_{in} - \sum W_{out} = g\frac{d(\rho V_0)}{dt} = g\rho\frac{dV_0}{dt} + gV\frac{d\rho}{dt}, \tag{3.59}$$

$$\sum W_{in} - \sum W_{out} = \frac{dV_0}{dt} + \frac{V_0}{\beta_e}\frac{dP}{dt}, \tag{3.60}$$

Applying the continuity equation to each of the piston chamber yields

$$Q_A - C_{ip}(P_A - P_B) - C_{ep}P_A = \frac{dV_1}{dt} + \frac{V_1}{\beta_e}\frac{dP_A}{dt}, \tag{3.61}$$

$$C_{ip}(P_A - P_B) - C_{ep}P_B - Q_B = \frac{dV_2}{dt} + \frac{V_2}{\beta_e}\frac{dP_B}{dt}, \tag{3.62}$$

where

V_1 : volume of forward chamber (including valve, connecting line and piston).

V_2 : volume of return chamber (includes valve, connecting line and piston).

C_{ip} : internal or cross-port leakage coefficient of piston.

C_{ep} : external leakage coefficient of piston.

β_e : bulk modulus obtained from general hydraulic fluid properties.

Considering no leakage flow in the cylinder,internal and external leakage coefficients equal to zero, the following equation can be obtained

$$Q_A = \frac{dV_1}{dt} + \frac{V_1}{\beta_e}\frac{dP_A}{dt}, \tag{3.63}$$

$$-Q_B = \frac{dV_2}{dt} + \frac{V_2}{\beta_e}\frac{dP_B}{dt}, \tag{3.64}$$

The volumes of the piston chambers may be written as:

$$V_1 = V_1' + A_1 x_p, \tag{3.65}$$

$$V_2 = V_2' - A_2 x_p, \tag{3.66}$$

where

A_p : area of piston

x_p : displacement of piston

V_1' : initial volume of forward chamber

V_2' : initial volume of return chamber

Using the previous volume of the piston chamber equations and assuming that $V_i' >> A_i x_p$, the continuity equations of each piston are

$$Q_A = A_1 \frac{dx_p}{dt} + \frac{V_1'}{\beta_e}\frac{dP_A}{dt}, \tag{3.67}$$

$$-Q_B = -A_2 \frac{dx_p}{dt} + \frac{V_2'}{\beta_e}\frac{dP_B}{dt}, \tag{3.68}$$

These equations relate the flow inside and outside the cylinder with the piston displacement and the pressure in both chambers. To simplify these two previous equations, some variables have to be predefined. These variables are the cylinder volume of the piston side V_1 and the cylinder volume of the piston rod side V_2. Firstly, piston areas have to be calculated depending on the piston and rod diameter:

$$A_1 = \frac{\pi\, d_p^2}{4}, \tag{3.69}$$

$$A_2 = \frac{\pi\, (d_p^2 - d_r^2)}{4}, \tag{3.70}$$

After that, initial volumes of both chambers are obtained based on the dead volume at the port i V_{i0}, the free length of the actuator l_{x0} and the length of the stroke l_c. Moreover, it is assumed that the cylinder is in the middle position. Using these parameters, Equations 3.65 and 3.66 can be rewritten as:

$$V_1' = V_{10} + \left(l_{x0} + \frac{l_c}{2}\right) A_1, \tag{3.71}$$

$$V_2' = V_{20} + \frac{l_c}{2} A_2, \tag{3.72}$$

The final equation arises by applying Newton's second law to the piston forces

$$F_{cyl} = A_1 P_A - A_2 P_B = M_t \frac{d^2 x_p}{dt^2} + B_p \frac{dx_p}{dt} + K_s x_p + F_L, \tag{3.73}$$

where

F_{cyl} : force generated or developed by piston

M_t : total mass of piston and load referred to piston

B_p : viscous damping coefficient of piston and load

K_s : load spring gradient

F_L : arbitrary load force on piston

This equation is used to obtain the relation between the force developed by the piston and both pressures in the cylinder. Doing a simplification of the system, viscous damping coefficient will be the only parameter that will affect the system. Moreover, F_{cyl} is obtained from the relation between the joint torques (mechanical dynamics) and hydraulic cylinder geometry, using the vector of generalized forces (Equation 3.46).

3.7 Relations between system variables

As explained earlier, each part of the system has its own modeling. Thus, to be able to design the controller of the forestry crane, all these models have to be included in a single one. To do so, every component of the machine has to be related to the rest of the components.

The forestry crane can be modeled in two different parts, which correspond to each hydraulic cylinder. The first hydraulic cylinder moves the second joint q_2 and the second cylinder moves the third joint q_3. It is important to remember that the first joint q_1 is fixed in the same position without movement around z-axis.

Each hydraulic system of the forestry crane parts is formed by a proportional valve and a hydraulic cylinder. These are the two blocks that will be included in Simulink to obtain the space-state equations of the system. The working principle of this hydraulic system is adding an input signal u, which is related to the spool displacement x_v, obtaining the hydraulic actuator displacement x_p. This displacement is able to move the forestry crane bodies getting different joint angles and thus, different Cartesian axis positions.

3.7.1 Proportional valve in the hydraulic system

The proportional valves used in the system are identical for each hydraulic system. The useful parameters to define this component in the modeling are the orifice flows Q_A,Q_B and the spool displacement x_v. These parameters were described in Equations 3.55, 3.56 and 3.57. The input parameter in the closed-loop control is the spool valve displacement x_v, which its transfer function is defined as

$$x_v = \frac{1}{\frac{1}{\omega_n^2}s^2 + \frac{2\xi}{\omega_n}s + 1}\,u, \tag{3.74}$$

The valve natural frequency used in the modeling is $\omega_n = 2\,\pi\,50\,\frac{rad}{s}$ and the valve damping ratio is $\xi = 0.8$. Another important parameter is the valve rated current, i.e., i_{rate}, that is used to normalize the input signal u. This parameter is taken as 1 mA and will be included as a gain in the modeling.

According to orifice flows, the values used for these parameters are the discharge coefficient $C_d = 1$, the diameter of the spool $d_{spool} = 10mm$ and the source and tank pressures $P_s = 150\ bar$ and $P_t = 0\ bar$ respectively.

The proportional valve block in Simulink (Figure 3.8) includes the transfer function and both orifice flow equations in each hydraulic cylinder. With the use of this block, flows Q_A and Q_B, which go to and come from the proportional valve respectively, are calculated. Inputs P_A and P_B are obtained from the hydraulic cylinder block explained below.

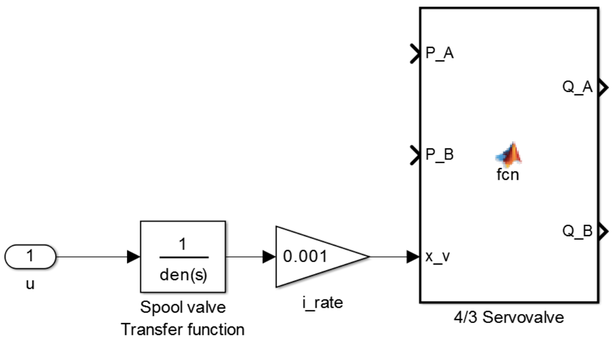

Figure 3.8 *Simulink block diagram of the proportional valve model*

3.7.2 Actuator in the hydraulic cylinder

Hydraulic cylinders used in the system are different in their design parameters. The equations which will be used in the modeling, are 3.67, 3.68 and 3.73. The continuity equations of each piston depends mainly on the dimensions of the piston, rod and stroke. Parameters and dimensions of both hydraulic cylinders are shown in Table 3.3, where the second column corresponds to the inner boom (first cylinder) and the third column corresponds to the outer boom (second cylinder).

	90x40-360 A590	80x40-420 A650
Piston diameter d_p (mm)	90	80
Rod diameter d_r (mm)	40	40
Length of stroke l_c (mm)	360	420
Dead volume V_{10} (mm^3)	50	50
Dead volume V_{20} (mm^3)	50	50
Viscous friction coefficient B_p $(N/(m/s))$	100	100

Table 3.3 *Dimensions and parameters of the hydraulic cylinders*

The equation related to the Newton's second law calculates the force exerted by the actuator rod F_{cyl} based on the areas and pressures in both chambers. In this equation, as is talked above, only viscous damping coefficient affects, obtaining the following equation:

$$F_{cyl_i} = A_{1i}P_{Ai} - A_{2i}P_{Bi} - B_{pi}\frac{dx_{pi}}{dt}, \tag{3.75}$$

F_{cyl} relates the body of the forestry crane with the hydraulic part of the system. Vector of generalized forces (Equation 3.46) is used to obtain this force. For the hydraulic cylinder, the force exerted by the hydraulic cylinder is calculated by using the derivative $J(q_i)$, as:

$$F_{cyl_i} = \frac{\tau_i}{J(q_i)}, \tag{3.76}$$

where τ_i and $J(q_i)$ are obtained from the mechanical dynamics (subchapter 3.4) and from the relation between d_{ci} and q_i (subchapter 3.5) respectively.

Although the force exerted by the actuator rod F_{cyl_i} depends on the joint angles q_i, it is considered constant in the Simulink modeling to obtain a simpler model equations. Once that this force is defined, it is possible to relate the proportional valve orifice flows Q_A, Q_B to the pressures in the chambers P_A, P_B and the piston displacement x_p in each hydraulic cylinder. The hydraulic cylinder parameters are obtained by using Equations 3.67, 3.68 and 3.75.. To obtain the variables from the derivative, integrator $1/s$ has to be used.

$$\dot{P}_B = -\frac{1}{K}\,q_B + \frac{A_2}{A_1}\frac{1}{K}\,q_A, \tag{3.77}$$

$$P_A = \frac{F_{cyl}}{A_1} + \frac{A_2}{A_1}\, P_B, \tag{3.78}$$

$$\dot{x}_p = -\frac{1}{A_1}\, q_A + \frac{V_1'}{\beta_e}\frac{A_2}{A_1^2}\, \dot{P}_B, \tag{3.79}$$

where K is a constant defined as

$$K = \frac{V_1'}{\beta_e}\frac{A_2^2}{A_1^2} + \frac{V_2'}{\beta_e}, \tag{3.80}$$

After the definition of these variables, it is possible to model the Simulink block. This block is shown in Figure 3.9 where P_A, P_B and x_p are obtained from Q_A and Q_B.

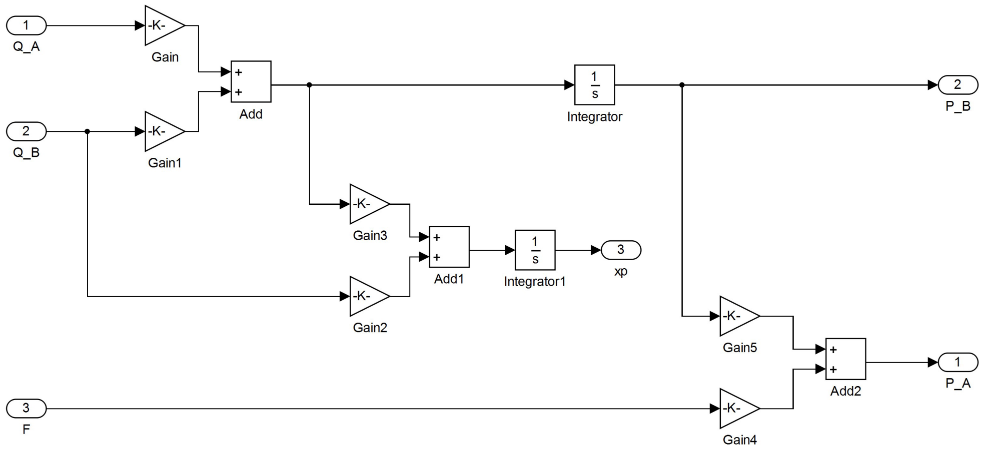

Figure 3.9 *Simulink block diagram of the cylinder model*

3.8 Control of the crane

In this section, control of the forestry crane is studied and explained. In order to achieve the objective of this Master's Thesis, once that modeling has been done, control is the next essential part to obtain the desired linear movement of the cutter. To do that, using the Simulink model explained in the previous sections, state-space of the system will be modeled to obtain the linear analysis of the system, which can consequently be used to tune the controller in the closed loop control afterwards.

3.8.1 Complete Simulink model and space-state

After designing the proportional valve and hydraulic cylinder blocks in Simulink, they have to be connected to be able to obtain the space-state linear model of the system. These blocks are connected as a closed loop control, using the output pressures of the hydraulic cylinder as inputs in the proportional valve block. The complete Simulink model is shown in Figure 3.10.

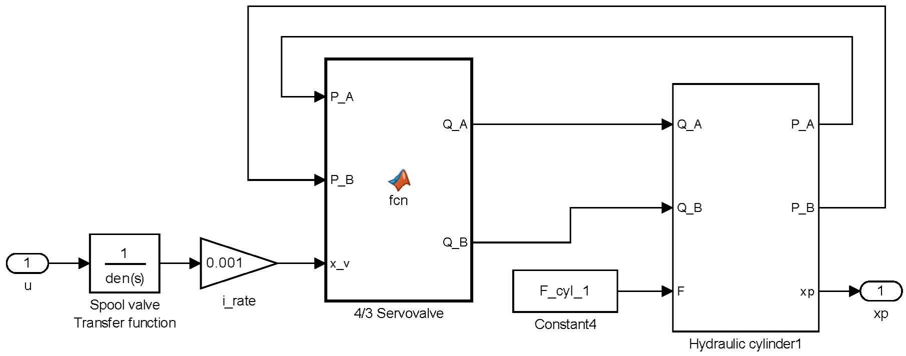

Figure 3.10 *Simulink block diagram of the hydraulic system model*

To obtain the space-state linear model, *linmod* function from MATLAB is used. This function gets the state-space linear model of the system of ordinary differential equations described in the block diagram.

State-space analysis is a method for describing the equations of motion for a dynamic system. This method can be used with both linear and nonlinear systems. However, to simplify the case of study, it will be done with linear time-invariant systems.

The state-space equations consist of state variables, input variables and output variables [9]. For this linear case, these variables are related to each other through the following state-space equations:

$$\dot{x} = Ax + Bu, \tag{3.81}$$

$$y = Cx + Du, \tag{3.82}$$

where x is a vector of state variables, u is a vector of input variables, y is a vector of output variables, A is called state matrix, B is called the input matrix , C is called the output matrix, and D is called the direct-transmission matrix.

These four space-state matrices are obtained from the MATLAB function and they are used to obtain the final transfer function of each hydraulic model of the forestry crane. It is important to define the input variable u as the proportional valve input signal u_i and the output variable y as the piston displacement x_p.

After these matrix definitions, it is possible to obtain the transfer function of the hydraulic system model. This continuous function relates the output of the system x_p to the input u_i. Moreover, it is calculated using the ss2tf function from MATLAB, which transforms the space-state matrices to continuous transfer function (Equation 3.83).

$$G_i(s) = \frac{numG_i(s)}{denG_i(s)} = C(sI - A)^{-1}B + D, \tag{3.83}$$

After the calculation of the transfer function in continuous-time, discretization has to be done in both of the cylinder models. This step means the transformation from continuous-time dynamic system to discrete time. To do that, the sampling time T is defined using the natural frequency of the proportional valve and the discretization method is Zero-older hold on the inputs (holding each sample value for one sample interval). Hence, it is possible to obtain the simulation as fixed steps and to have a digital signal through the closed-loop control. This digital signal is an important part for the implementation in the real forestry machine.

Finally, using all parameters of the system (mechanics and hydraulics), two different discrete-time transfer functions are obtained. These functions depend on which hydraulic system has been modeled. Thus, it is possible to tune the controller of the intelligent control system.

3.8.2 PI Control

After discretization of the model transfer function, controller can be tuned to obtain the desired output signal in a closed-loop control. This control is shown in the figure 3.11 using Simulink blocks and having the piston displacement dc_i as a reference obtained from a desired Cartesian position $[X, Y]$.

In this closed-loop, the reference position of the hydraulic cylinder is calculated for $q_2 = 0^o$ and $q_3 = -90^o$. Having a reference position dc_2, the controller has to be tuned to obtain the minimum error at the permanent state. This controller attempts to minimize the error by adjusting of a control variable determined for a

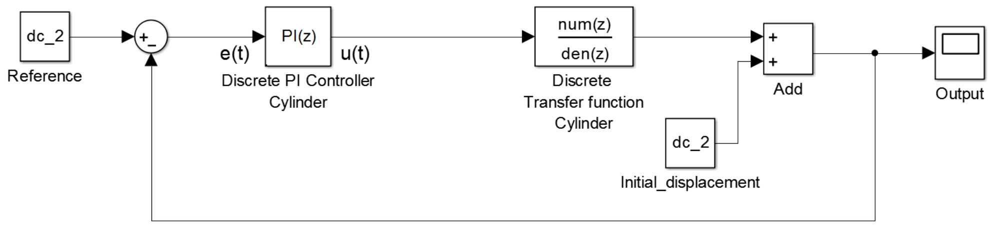

Figure 3.11 *Simulink block diagram of the closed loop control model*

Proportional-integral-derivative controller by the sum:

$$u(t) = K_p\, e(t) + K_i \int_0^t e(\tau) d\tau + K_d\, \frac{de(t)}{dt}, \tag{3.84}$$

with its Laplace transformation:

$$u(t) = K_p\, e(t) + K_i \frac{1}{s} + K_d s, \tag{3.85}$$

where u(t) is the output signal of the controller, e(t) is the error signal of the control and K_p, K_i, K_d denote the coefficients for the proportional, integral and derivative terms respectively.

Proportional-Integral (PI) controller is used in this modeling of the forestry crane because simple controllers are always the easiest way to implement in real applications. Proportional controller would be the simplest controller that can be used in this closed-loop control. However, P controller does not cancel the permanent error in the output signal. Therefore, PI is the suitable controller for this application. The contribution of the integral term is proportional to the magnitude and the duration of the error. Using this controller, error position is zero (permanent is guaranteed) and transitory can be improved, hence increasing the gain. For a discrete-time parallel PI controller, using Equation 3.85, the transfer function takes the form

$$C(z) = K_p + K_i \frac{T_s}{z - 1}, \tag{3.86}$$

where Forward Euler is the integrator method for the discrete-time settings for a sampling time of $T_s = 0.02s$. Controller parameters K_p and K_i are defined based on the response time and the transient behavior. Increasing the response time and the transient behavior improves stability and reduces overshoot in the tracking response, although leading to longer settling time. Due to the fact that a robust controller is required for this application, both of these last parameters are high in comparison to the ideal parameters. Due to that, closed-loop control will response suitably versus any disturbance related to non-linearities. A maximum transient behaviour 0.9 and a response time of T = 0.5 sec is used.

Using these assumptions, PI controllers in both hydraulic system have the following parameters:

	PI First Cylinder	PI Second Cylinder
Proportional Gain K_p	5.1102	6.9067
Integral Gain K_i	0.35769	0.48344

Table 3.4 *Parameters of the Proportional-Integral controller*

3.8.3 Performance of the controller

Once the PI controllers have been designed with suitable parameters for the system, plots and diagrams can be used to analyze the closed-loop response in the presence of a reference signal.

In the figure 3.12, system modeling in Simulink is shown with both PI controllers included. In this design, the references of the system are the Cartesian coordinates of the grapple point ($X_{grapple}$ and $Y_{grapple}$ as shown in figure 2.6). Due to the relation between Cartesian coordinates and joint angles defined in the section 3.2, q_2 and q_3 are obtained. After that, hydraulic cylinder displacement is defined by these joint angles (section 3.5), being the reference of the closed-loop control.

Some useful results can be obtained from this model. Signal outputs show how the system responds from the initial position to the desired one. Moreover, Bode plot from the control design is used to know the oscillation and the time response of the controller according to the control parameters K_p and K_i.

Results for both PI controllers are bode plots for open loop, R-locus for open loop and step response. For the PI controller in the first hydraulic cylinder, these plots are shown in figures 3.13, 3.14 and 3.15 respectively.

In the Bode plot of the Figure 3.13 it is possible to see which order system is, using magnitude and phase plot. Moreover, depending on the gain of the system, stability

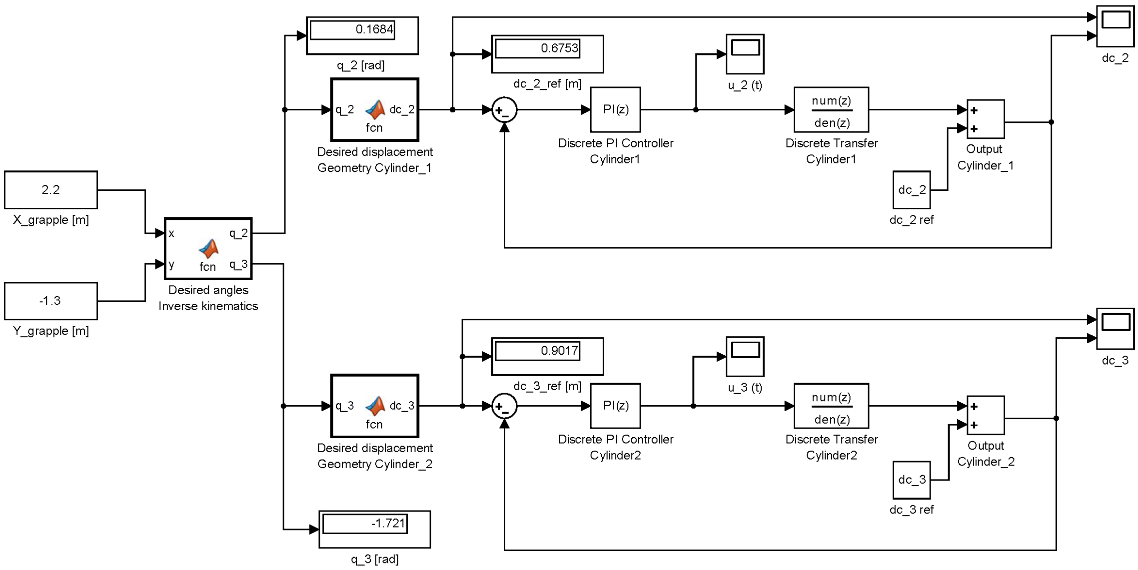

Figure 3.12 *Simulink block diagram of the complete system model*

and oscillations of the response vary. In this case, due to the fact that controller has been defined following robust parameters, phase margin is close to 90 degrees and gain margin is negative. If system gain would be increased, time response would be decreased having higher oscillations in the response. If system gain is increased enough, the system can be unstable.

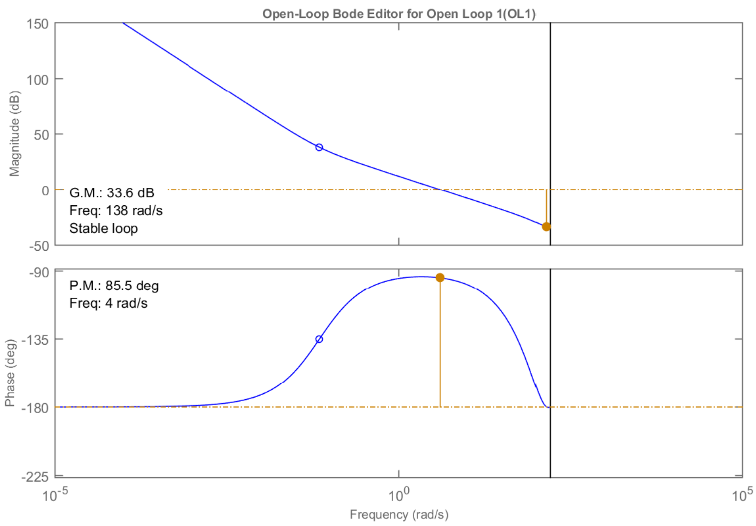

Figure 3.13 *Bode plot for open loop in the first hydraulic cylinder*

The root locus can be used for the analysis of the stability in discrete time. In this situation, the stability condition is that every root has to be $|z_i| < 1$. As it is shown in Figure 3.14, every root in this system are inside the circle of radius $z = 1$, demonstrating the stability of the system.

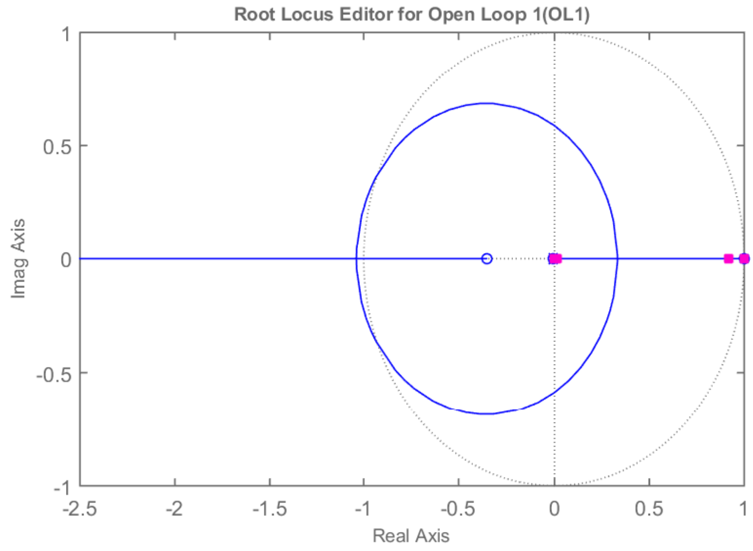

Figure 3.14 *Rlocus for open loop in the first hydraulic cylinder*

Another possibility to see how stable and how much error positioning the system has is having a step as an input signal of the close-loop control. As it can be seen in Figure 3.15, there is not any oscillation and the error position in the permanent state is not significant even though the time response is higher in comparison with controllers with higher damping ratio. It means that these controllers have a robust and stable output response. In these cases, the hydraulic cylinder goes from the initial position $dc_{2,ref}$ and $dc_{3,ref}$ in $[X_{grapple} = 2.2\ m, Y_{grapple} = -1.669\ m]$ to the desired actuator displacement in $[X_{grapple} = 2.2\ m, Y_{grapple} = -1.3\ m]$.

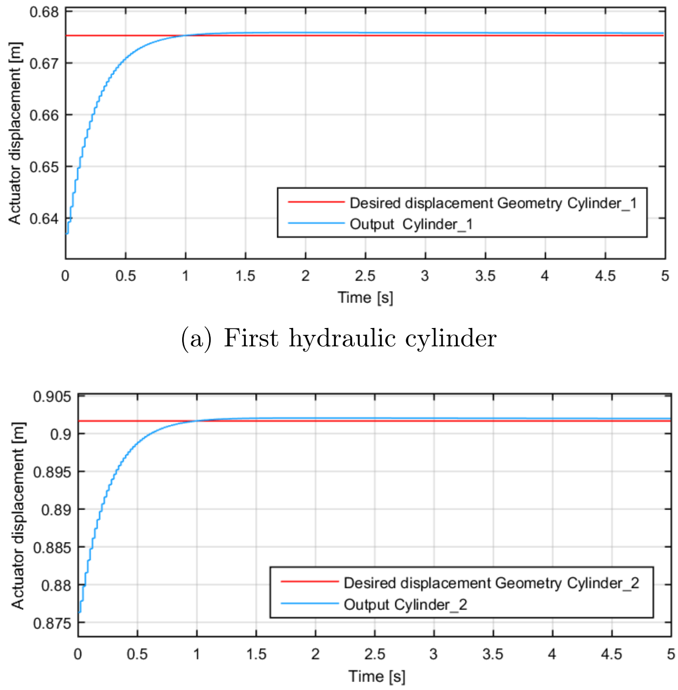

(a) First hydraulic cylinder

(b) Second hydraulic cylinder

Figure 3.15 *Output vs desired displacement in the hydraulic cylinders*

4. SIMULATION OF THE CRANE CONTROL USING AMESIM

4.1 Software description

LMS Imagine.Lab AMESim is the simulation software used in this Master's Thesis. AMESim is a platform for modeling, simulation and analysis of multi-domain controlled systems, being part of systems engineering domain and it is categorized as mechatronic engineering field. Moreover, this software provides libraries for different engineering fields such as fluids, thermodynamics, electromechanical, mechanical or signal processing among others [14].

AMESim software is used instead of MATLAB/Simulink due to the fact that there is a possibility to easily include non-linearities of the hydraulic components in the simulation. These non-linearities have been avoided in the system modeling to simplified the equations. Moreover, there are more advantages using an advanced modeling and simulation tool instead of MATLAB/Simulink, i.e. forestry crane arms can be included as rigid bodies and perfect joints, possibility to obtain a 2-Dimensions simulation or the ease to obtain plots and result variables from the machine components.

4.2 Component descriptions

Following the sections described in Chapter 3, the simulation model is designed using three different parts: mechanical, control and hydraulic. The circuit schematic includes submodels from AMESim library, in which the MATLAB parameters and machine dimensions are defined. These component submodels are generally descrived in Appendix B.

4.2.1 Hydraulic submodels

Hydraulic model has the components described in section 3.6. These components are proportional valve, hydraulic cylinder, hydraulic pipes or hoses, hydraulic pressure source and tank. In the real forestry machine, load-sensing system (LS) is used with an axial piston variable pump (see Figure 4.1). The variable displacement pump delivers only the volume required at any given moment and the supply pressure is limited using a pressure relief valve. Moreover, there is a electro-proportional control with controller cut-off which is able to vary the pump volumetric displacement.

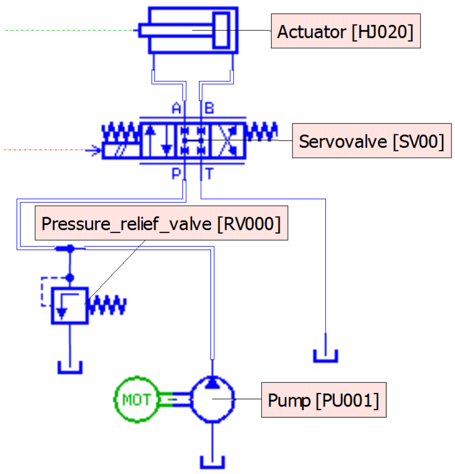

Figure 4.1 *Hydraulic AMESim model in the real machine*

In this Master's Thesis, a simplification of the system has been done in the hydraulic schematic, more specifically in the pressure source. As was explained above, the pressure source is limited by the pressure relief valve. To have a constant value of the pressure source, these hydraulic components have been replaced by a constant pressure source P_s with value 150 bar. This simple schematic is shown in Figure 4.2. The same simplification has been done in the system modeling, so hydraulic dynamics are similar in both cases.

Finally, submodel parameters, described in 3.6, are defined following the same assumptions than system modeling. However, due to the fact that non-linearities are included in this simulation software, the mathematical expressions which define connections between components and the proportional valve are different than system modeling.

The hydraulic pipes are defined depending on the position as a direct connection

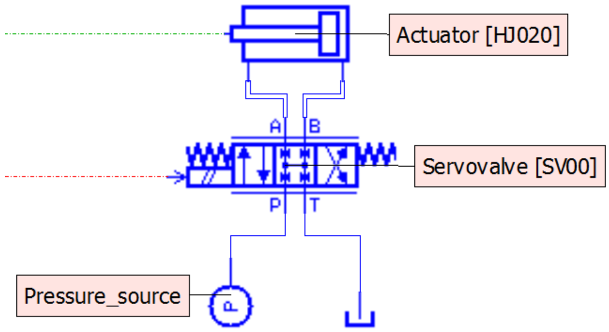

Figure 4.2 *Hydraulic AMESim model simplified*

or compressibility + friction hydraulic line (C-R). The difference between them can be seen in the Appendix B. C-R hydraulic line parameters are compressibility and friction:

- Compressibility: The compressibility of the fluid and expansion of the pipe wall with pressure are taken into account by using an effective bulk modulus. It is calculated based on the wall thickness and Young's modulus for the wall material. In this simulation, Young's modulus for material is 50.000 bar and wall thickness is 1.245 mm (from SCH 5s [21]).

- Friction: Pipe friction is taken into account using a friction factor based on the Reynolds number and relative roughness.

There are two different C-R hydraulic lines, type 1 from pressure source to the proportional valve and type 2 and 3 from proportional valve to actuator in the first and second hydraulic cylinder respectively. These line parameters are shown in 4.1.

	Type 1	Type 2	Type 3
Pipe diameter $d_{pipe}[mm]$	18.00	10.00	10.00
Pipe length $L_{pipe}[m]$	0.50	2.00	4.00

Table 4.1 *Parameters of the C-R hydraulic lines*

In the case of the proportional valve, two AMESim utilities are used to define the orifice area *areap* and the flow rates Qa and Qt. The equivalent area and hydraulic diameter, which satisfy a giving pressure drop ΔP and a volumetric flow rate Q, are estimated solving the following equation, similar than Equation 3.47.

$$q = A\, c_{qmax} \sqrt{\frac{2\Delta P}{\rho}} \tanh\left(\frac{2\, d_{spool}\sqrt{\frac{2\Delta P}{\rho}}}{\nu\, \lambda_c}\right), \tag{4.1}$$

where

ρ : density of hydraulic fluid $[kg/m^3]$

Q : flow rate $[m^3/s]$

ΔP : corresponding differential pressure $[Pa]$

c_{qmax} : maximum flow coefficient

ν : kinematic viscosity of hydraulic fluid $[m^2/s]$

λ_c : critical flow number (transition between laminar and turbulent flow)

Flow rate through an orifice Q and the corresponding flow coefficient c_p and flow number λ are also calculated in this proportional valve [10].

In addition to that, friction evaluation is an essential part in a hydraulic system. Friction affects in the hydraulic system in two different components: hydraulic lines and hydraulic cylinders.

- Hydraulic lines: As it is explained above, C-R hydraulic lines are used and the friction is calculated based on the Reynolds number and relative roughness.
- Hydraulic cylinder: Viscous friction and leakage coefficient are the parameters related to friction. In this case, assuming that leakage coefficient is zero, only viscous friction coefficient B_p affects the hydraulic system friction evaluation.

4.2.2 Signal and control submodels

Control components are shown in Figure 4.3. An important component is the Simulink to AMESim block, where the forestry crane kinematics and the geometric direct model are included. Using this block and having $[X_{grapple}, Y_{grapple}]$ as an input value, the hydraulic cylinder displacement related to each point of the trajectory can be obtained. As it can be seen in Figure 4.3, there are two constant signals called Offset.cyl.1 and Offset.cyl.2. These components are used to compensate the free length of the actuator in the translational actuator submodel.

Once that this displacement is defined, the feedback signal in the closed-loop control is obtained using a sensor displacement in the hydraulic cylinder. This sensor gets the position of the actuator at each moment. As a consequence, the trajectory of the cutter is transferred to hydraulic displacement, facilitating the reference signal in the closed-loop control.

After obtaining the error signal from the difference between reference and feedback signal, it is transformed to the action through the PI controller. Finally, the PI output is sent to the proportional valve as u variable.

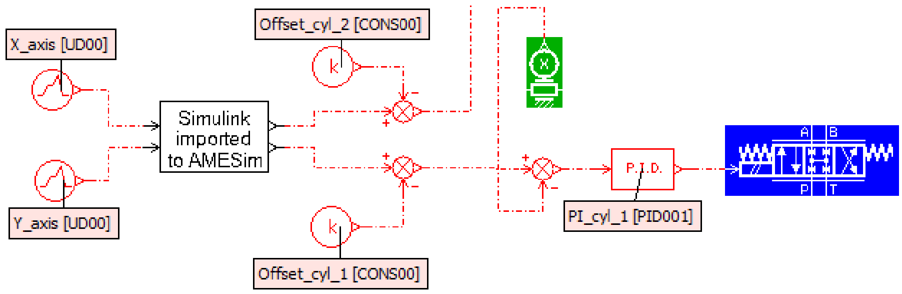

Figure 4.3 *Control AMESim model*

4.2.3 Mechanical submodels

Mechanical schematic is built using Planar mechanical submodels as body parts, joints and translational actuators. Body parts are defined using the same machine dimensions and specifications are described in section 3.2 and shown in Table 4.2. Translational actuator parameters are defined following the hydraulic cylinder characteristics described in section 3.6.

Component	Dimension $[m]$	Mass $[Kg]$
Body 2	$L_2 = 2.200$	73.70
Body 3	$L_3 = 1.669$	49.20
Body 4	$L_4 = 0.273$	5.00
Body 5	$L_5 = 0.270$	5.00
Body G	$r_G = 0.200$	189.00

Table 4.2 *Parameters of the mechanical AMESim model*

4.2.4 Complete model

The complete schematic using the components described above is shown in Figure 4.4. All submodels described above are included. Moreover, using PLM assembly, the parametrization and the simulation animation of the planar system is visualized. This animation of the simulation run is shown in Figure 4.5, where all planar mechanical submodels are included.

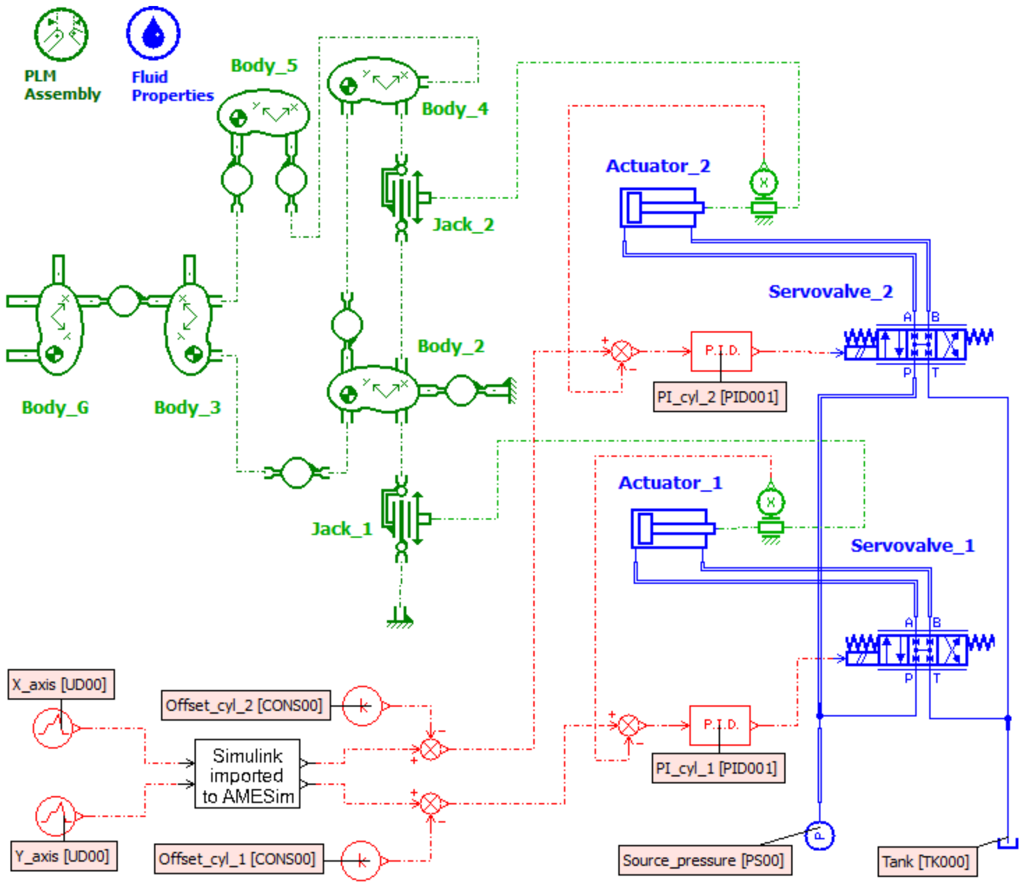

Figure 4.4 *AMESim block diagram of the complete model*

4.3 Simulation results

Two different simulations have been done in AMESim Software. Both of them earn the same positions, however, the input signals are different. As it has been explained in earlier chapters, the aim of this Master's Thesis is the obtaining of a simple controller which is able to control the boom operations, having a linear trajectory of the forestry crane. The controller has been tuned using Simulink tool and the linear trajectory is obtained using a linear signal source. Desired $[X_{grapple}, Y_{grapple}]$ positions are these signal source stages making a linear trajectory.

The first simulation is done with a step signal and it is compared with the controller performance obtained from Simulink. In the second one, the input signal is a ramp with the same values than the previous trajectory. These positions of the trajectory are shown in Table 4.3 and Figure 4.6. These points are reached separately having enough time to stabilize the forestry crane. To obtain the permanent state, the time

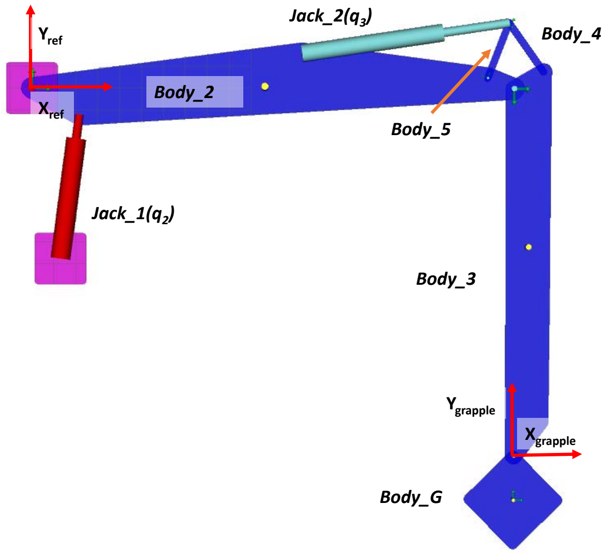

Figure 4.5 *Planar animation of the forestry crane at initial position*

simulation is 40 seconds in both cases.

Position	$X_{grapple}$ $[m]$	$Y_{grapple}$ $[m]$
Initial value	2.200	-1.669
Point 1	2.200	-1.400
Point 2	3.000	-1.400

Table 4.3 *Points of the forestry crane trajectory*

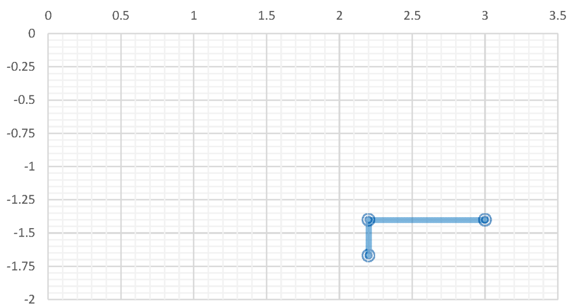

Figure 4.6 *Forestry crane trajectory*

4.3.1 Step response simulation

Once that the forestry crane trajectory has been defined, it is possible to obtain some relevant simulation results to know how the system response. In this first simulation, a step response in the input signals is introduced. Due to the fact that the step function is the fastest way to reach the next point in the trajectory, minimum time response in the simulation is studied. Moreover, it is possible to compare this simulation with Simulink results.

The accurate of the control system is measured in the Figure 4.7. Comparison of desired forestry crane trajectory and simulation results shows that error position is not relevant. As it can be seen in these plots, the maximum error is produced while the forestry crane is going to the next step in the trajectory. In the permanent state, this Y-axis error position is approximately 2 cm, which is an insignificant value in this forest industry.

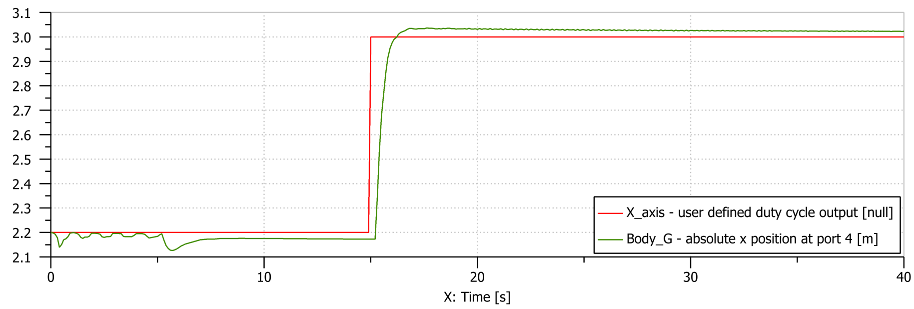

(a) $X_{grapple}$

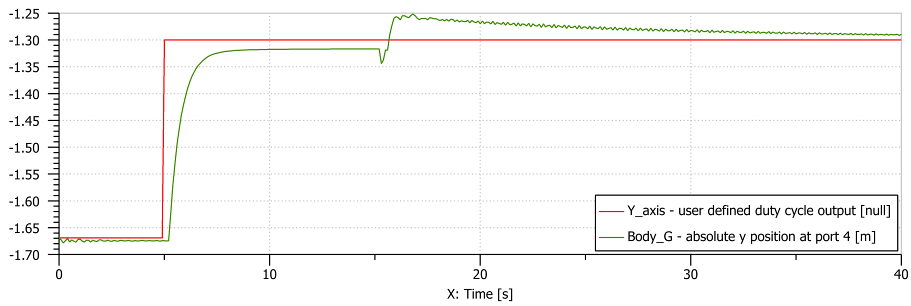

(b) $Y_{grapple}$

Figure 4.7 *Comparison of desired and simulated $X_{grapple}$, $Y_{grapple}$ in step function*

Another simulation result to test the accuracy of the system is the comparison of reference and simulation piston displacements. As it can be seen in Figure 4.8, the accuracy of the system is suitable for the application, reaching approximately the given point. Despite of the fact that time response of the system is higher than Simulink model, it is still suitable for this case, being less than 1.5 sec.

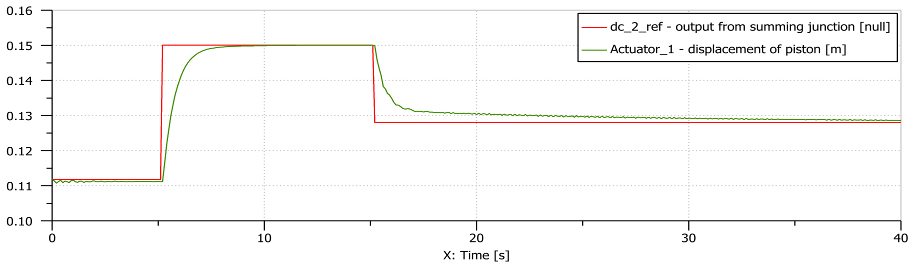

(a) First hydraulic cylinder

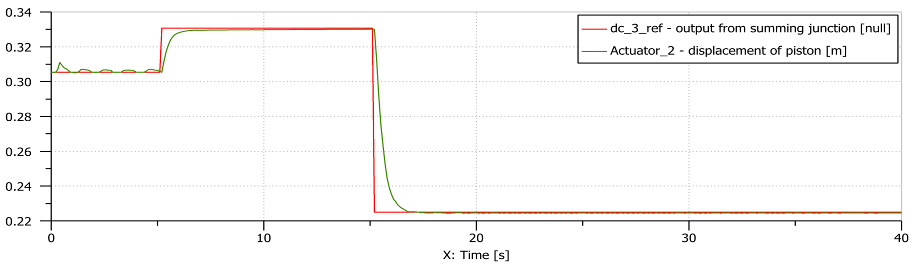

(b) Second hydraulic cylinder

Figure 4.8 *Comparison of desired and simulated piston displacement in step function*

According to the proportional valve results, it is possible to see how the system works with the input signal obtained from the PI controller. In the Figure 4.9, three different plots are shown from the proportional valve of the first hydraulic cylinder. The flows through the proportional valve vary according to spool displacement. This spool displacement is directly proportional to the output from PI controller. In the third plot, it is possible to see how the first actuator piston displacement vary with the spool displacement.

Friction evaluation is an essential variable in this simulation. As it was explained in the hydraulic submodel, the components which include friction are hydraulic lines and hydraulic cylinders. However, actuators are the main component in this friction study. According to the application of Newton's second law to the piston forces (Equation 3.73), there are four different parameters which affect on the force developed by piston F_{cyl}. In this case of study, the viscous damping coefficient B_p and the actuator piston velocity $\dot{x}_p$ produces a friction force opposite to F_{cyl}. The maximum $\dot{x}_p$ is 0.08 m/s, moment that actuators are moving from Point 1 to Point 2. Using hydraulic cylinder values described in the Table 3.3, B_p is equal to 100 N/(m/s). It means that the maximum friction force is 8 N, which is small

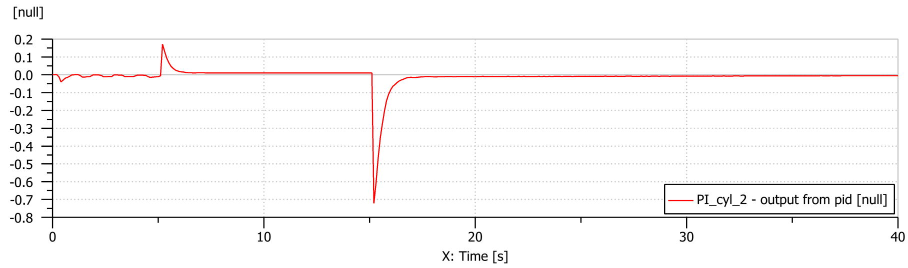

(a) PI controller output signal

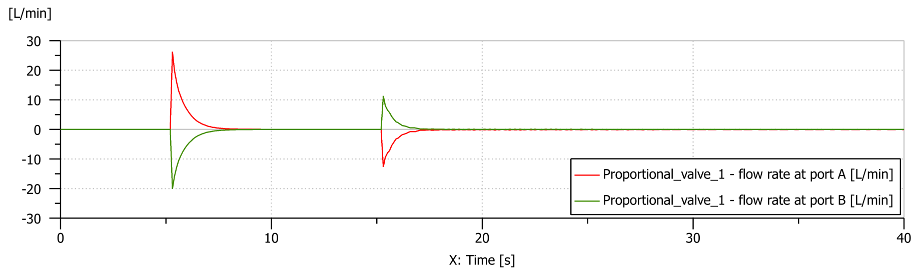

(b) Flow rate at port A and B in proportional valve

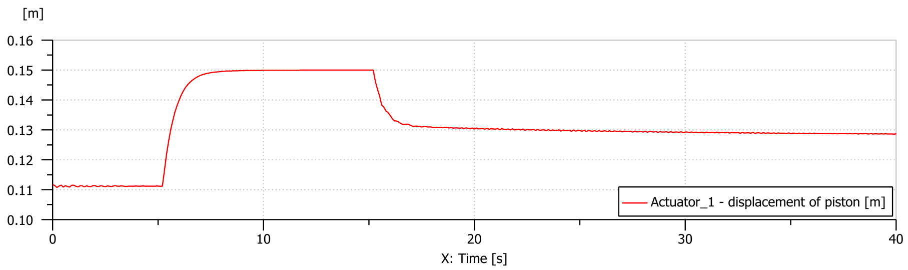

(c) Piston displacement in the first hydraulic cylinder

Figure 4.9 *First actuator results from the simulation*

compared with the force exerted by actuator rod F_{cyl} at the same time (30.000 N). As a consequence, the friction in this simulation is not a relevant variable to be considered.

4.3.2 Ramp function simulation

Ramp function is better for the forestry crane working performance. This is due to the piston displacement can vary linearly having a soft slope. The error position is still not relevant, as it can be seen in the Figure 4.10. In addition, despite the time response, the trajectory created with ramp function allow the obtaining of a safe response. The linear piston displacement can be seen in the Figure 4.11.

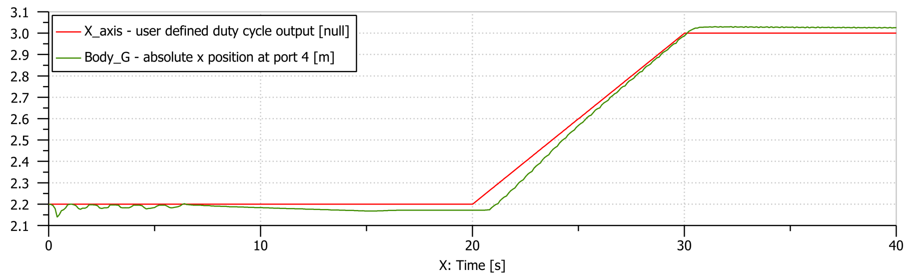

(a) $X_{grapple}$

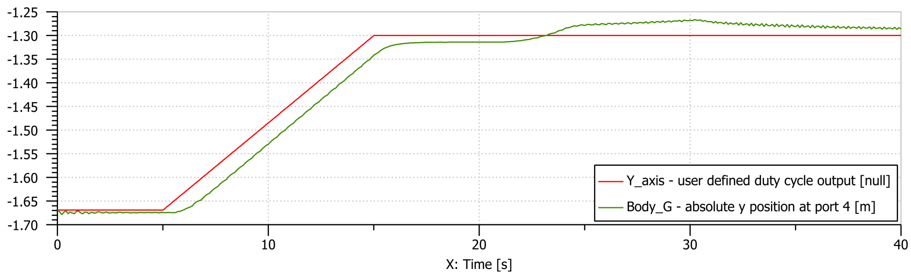

(b) $Y_{grapple}$

Figure 4.10 *Comparison of desired and simulated* $X_{grapple}$, $Y_{grapple}$ *in ramp function*

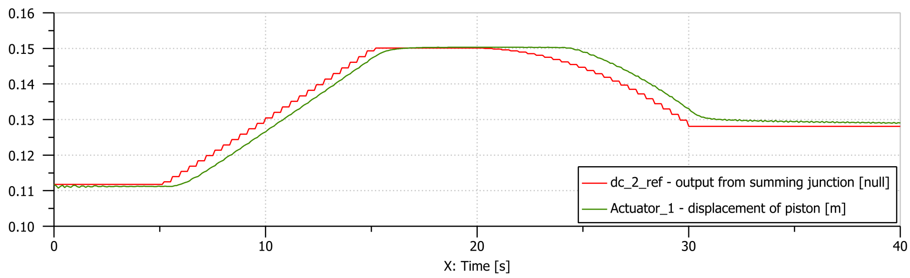

(a) First hydraulic cylinder

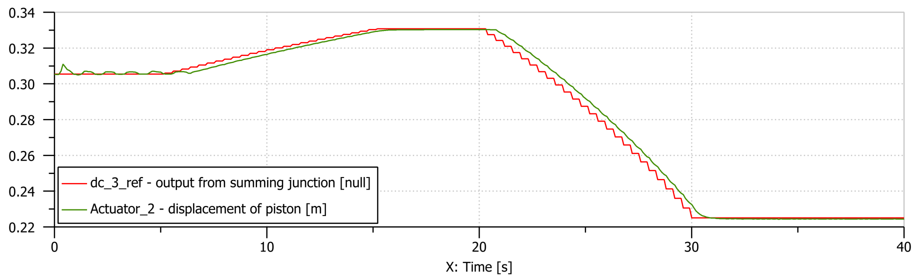

(b) Second hydraulic cylinder

Figure 4.11 *Comparison of desired and simulated piston displacement in ramp function*

5. DISCUSSION

Once the simulation results have been obtained from an advanced modeling and simulation tool, it is possible to verify the accuracy and repeatibility of the system. As it was explained in the step and the ramp function results, the error position using a simple controller is not relevant due to the fact that it is approximately 2 cm in Y-axis. Moreover, the time response in the ideal situation (step function) is correct enough for the application in study.

In spite of the fact that every part and component of the real machine has been studied in modeling and simulation, some simplification of the system have been done along this Master's Thesis. As a consequence, it would be important to include the same configuration in the simulation than the real machine such as pressure source configuration and the movement in z-axis of the first joint q_1. These two simplifications, as previously explained, have been done to obtain a similar simple model in MATLAB/Simulink and AMESim software.

Due to the simplification in the pressure source configuration, there are some important variations in the flow rates and pressures included in hydraulic system. In a future study, every component from the Load-sensing system has to be included to analyze how the system response with. It means that pressure relief valve, axial piston variable pump and the electro-proportional control with controller cut-off are components of the real hydraulic AMESim model. Moreover, it means that non-linearities are completely studied, obtaining an accurate results of the forestry crane.

According to the forestry crane structure, only two joint angles are controlled in this Master's Thesis: inner boom q_2 and outer boom q_3. The slewing q_1 is defined as a fixed value to obtain a 2-Dimension movement. Nevertheless, the complete work space in an articulated manipulator includes three-jointed structures q_1, q_2 and q_3. As it can be seen in the Figure 2.3, the complete forestry machine work space involve a 3-D movement. Including this slewing joint angle in the controller, every point of the work space would be accessible.

However, this intelligent control system is good enough to be implemented in the real machine. As it has been studied in the simulations, accuracy, pressure and flow rates and piston displacement in both actuators are within the operating range of the components used. In addition, Proportional-Integral controller is simple and easy to included in an integrated circuit.

6. CONCLUSIONS

The main purpose of this thesis was the obtaining of a modern control system which will be able to help the driver in the cutting actions. This intelligent control system is able to create a linear trajectory of the cutter in the forestry crane. This linear trajectory enhance the working efficiency and reduce the human interaction.

As a start to the control system design, every part of the forestry crane has been modeled in MATLAB/Simulink. Some small assumptions have been done to try to keep the mathematical expressions rather simple. In this model, kinematics are approximate to articulated manipulator with two revolute joints. Moreover, mechanical and hydraulic dynamics are studied to include in Simulink blocks. These Simulink model is used to tune the controller of the closed-loop system. To simplify this intelligent control system, Proportional-Integral controller has been introduced in the system. Modeling and simulation are done following dimensions and parameters from Usewood Pro small harvester. As a consequence, every plot and result has been tested to ensure the operating range of the components.

LMS Imagine.Lab AMESim is used to run the simulation of the system. This advanced simulation tool includes non-linearities of the hydraulic components in the simulation. Furthermore, it is possible to obtain a 2-Dimensions simulation or the ease to obtain plots and result variables from the system components.

Using this advanced simulation tool, the modern control system response has been studied. According to inverse kinematics and geometry of the forestry crane, piston displacements can be defined. The movement of the forestry crane is done with different desired points following a linear trajectory. The accuracy and the repeatability of the control system is good enough for the forest applications.

Future research topics in this topic could include the whole Load-sensing system in the hydraulic system and the slewing movement in the forestry crane. These two topics bring the simulation closer to the real forestry machine. The final step in this

Master's Thesis topic will be the implementation in the real forestry machine.

BIBLIOGRAPHY

[1] J. J. Craig, *Introduction to Robotics: Mechanics and Control*, 3rd ed. Prentice Hall, 2005.

[2] J. Denavit and R. Hartenberg, "A kinematic notation for lower-pair mechanisms based on matrices," *Journal of Applied Mechanics*, pp. 215–221, Jun. 1955.

[3] A. Heinze, "Modelling, simulation and control of a hydraulic crane," M.S.M.E. thesis, Munich University of Applied Sciences, September 2007.

[4] P. L. Hera and D. O. Morales, "Modeling dynamics of an electro-hydraulic servo actuated manipulator: a case study of a forestry forwarder crane," *Procedings of the World Automation Congress (WAC'12)*, pp. 1–6, June 2012.

[5] ——, "Model-based development of control systems for forestry cranes," *Journal of Control Science and Engineering, Hindawi Publishing Corporation*, vol. 2015, May 2015.

[6] P. L. Hera, B. U. Rehman, and D. O. Morales, "Electro-hydraulically actuated forestry manipulator: Modeling and identification," *Proceedings of the 25th IEEE/RSJ International Conference on Intelligent Robots and Systems (IROS '12)*, pp. 3399–3404, October 2012.

[7] P. X. M. LaHera, U.Mettin, I.Manchester, and A. Shiriaev, "Identification and control of a hydraulic forestry crane," *Proceedings of the 17th World Congress, International Federation of Automatic Control (IFAC'08)*, pp. 2306–2311, July 2008.

[8] R. Liu, "Nonlinear control of electro-hydraulic servosystems: theory and experiment," M.S.M.E. thesis, University of Illinois, Urbana, Illinois, 1994.

[9] N. D. Manring, *Hydraulic control systems*, 1st ed. John Wiley and Sons, 2005.

[10] D. McCloy and H. Martin, *Control of Fluid Power : Analysis and design*, 2nd ed. Ellis Horwood Limited, 1980.

[11] H. E. Merritt, *Hydraulic Control Systems.* John Wiley and Sons, 1967.

[12] D. O. Morales, S. Westerberg, P. X. L. Hera, U. Mettin, L. Freidovich, and A. S. Shiriaev, "Increasing the level of automation in the forestry logging process with crane trajectory planning and control," *Journal of Field Robotics*, vol. 31, no. 3, pp. 343–363, May/Jun. 2008.

[13] S. Noack, *Hydraulics in mobile equipment*, 2nd ed. Bosch Rexroth AG didactic, 2001.

[14] *LMS Imagine.Lab Amesim Brochure*, Siemens PLM Software, 2016, Available: https://www.plm.automation.siemens.com/en_us/products/lms/imagine-lab/amesim/index.shtml [Jul. 04, 2016].

[15] M. W. Spong, S. Hutchinson, and M. Vidyasagar, *Robot Modeling and Control*, 1st ed. John Wiley and Sons, 2006.

[16] B. Sulc and J. A. Jan, "Non linear modelling and control of hydraulic actuators," *Acta Polytechnica*, vol. 42, no. 3, pp. 41–47, 2002.

[17] S. Tafazoli, P. D. Lawrence, S. E. Salcudean, D. Chan, S. Bachmann, and C. E. de Silva, "Parameter estimation and actuator friction analysis for a mini excavator," *Proceedings or the 1996 IEEE International Conference on Robotics and Automation*, pp. 329–334, April 1996.

[18] S. Tafazoli, S. E. Salcudean, K. Hashtrudi-Zaad, and P. D. Lawrence, "Impedance control of a teleoperated excavator," *IEEE Transactions on control system technology*, vol. 10, no. 3, pp. 355–367, May 2002.

[19] Usewood.Forest.Tec.Oy, *Usewood Forest Master*, Muurame, Finland, 2016, Available: http://www.usewood.fi/images/pdf/Usewood_Forest_Master.pdf [Jun. 22, 2016].

[20] ——, *Usewood Forest Master: Features*, Muurame, Finland, 2016, Available: http://www.usewood.fi/images/pdf/Features_051015_ENG.pdf [Jun. 22, 2016].

[21] Wikipedia, *Nominal pipe size*, 2016, Available: https://en.wikipedia.org/wiki/Nominal_Pipe_Size#cite_note-DN-2 [Jul. 04, 2016].

APPENDIX A. MATLAB CODE WITH FORESTRY CRANE PARAMETERS

```
%-----------------------------------------------------------------------%
%---------------------------- Fluid properties -------------------------%
%-----------------------------------------------------------------------%
%Bulk modulus
beta_e = 17000; %bar
beta_e = beta_e * 1e+5; %Pa
%Density
rho = 850; %kg/m^3

%-----------------------------------------------------------------------%
%-------------------- Parameters of the forestry crane -----------------%
%-----------------------------------------------------------------------%
%Masses
m_2 = 73.7; %kg
m_3 = 41.8 + 7.4; %kg
m_G = 155 + 34; %kg
g = 9.81;
%Lengths
L_2 = 2.2; %m
L_3 = 1.669; %m
r_G = 0.2; %m
Lc_2 = 1.064; %m
Lc_3 = 0.570; %m
%Inertias
I_2 = 1/12*m_2*L_2^2;
I_3 = 1/12*m_3*L_3^2;
I_G = 1/2*m_2*r_G^2;

%-----------------------------------------------------------------------%
%---------------Variables of hydraulic cylinder geometry----------------%
%-----------------------------------------------------------------------%
%First hydraulic cylinder geometry
beta_1 = sin(0.1305/0.787); %rad
beta_2 = tan(0.120/0.217); %rad
l_1 = 0.787; %m
l_2 = sqrt(0.120^2 + 0.217^2); %m
%Second hydraulic cylinder geometry
```

```
beta_3 = deg2rad(6); %rad
beta_4 = 0.48; %rad
beta_5 = deg2rad(22); %rad
beta_6 = deg2rad(180 - 90 - 22); %rad
beta_7 = 0.547; %rad
l_3 = 0.130; %m
l_4 = 0.155; %m
l_5 = 0.270; %m
l_6 = 0.273; %m
l_7 = 0.855; %m

%-------------------------------------------------------------------------%
%------------------- Hydraulic parameters - First Cylinder ---------------%
%-------------------------------------------------------------------------%
%Dead volume at port end
V_10_1 = 50*1e-6; %m^3
V_20_1 = 50*1e-6; %m^3
%Length of stroke
l_c_1 = 0.420; %m
%Initial displacement of the actuator
l_c_0_1 = l_c_1/2; %m
%Free length of the actuator
l_x_0_1 = 0.650; %m
%Piston and rod diameter
d_p_1 = 0.080;%m
d_r_1 = 0.040;%m
%Piston area
A_1_1 = pi/4*(d_p_1)^2; %m^2
%Ring area = piston area - rod area
A_2_1 = pi/4*(d_p_1^2 - d_r_1^2);
%Cylinder volume of the piston side
V_1_1 = V_10_1 + (l_x_0_1 + l_c_0_1)*A_1_1;
%Cylinder volume of the piston rod side
V_2_1 = V_20_1 + l_c_0_1*A_1_1;

%-------------------------------------------------------------------------%
%------------------- Hydraulic parameters - Second Cylinder --------------%
%-------------------------------------------------------------------------%
%Dead volume at port end
V_10_2 = 50*1e-6; %m^3
V_20_2 = 50*1e-6; %m^3
%Length of stroke
l_c_2 = 0.360; %m
%Initial displacement of the actuator
```

```
l_c_0_2 = l_c_2/2; %m
%Free length of the actuator
l_x_0_2 = 0.550; %m
%Piston and rod diameter
d_p_2 = 0.090;%m
d_r_2 = 0.040;%m
%Piston area
A_1_2 = pi/4*(d_p_2)^2; %m^2
%Ring area = piston area - rod area
A_2_2 = pi/4*(d_p_2^2 - d_r_2^2);
%Cylinder volume of the piston side
V_1_2 = V_10_2 + (l_x_0_2 + l_c_0_2)*A_1_2;
%Cylinder volume of the piston rod side
V_2_2 = V_20_2 + l_c_0_2*A_1_2;

%------------------------------------------------------------------------%
%------------- Spool valve parameters- First cylinder -------------------%
%------------------------------------------------------------------------%
%Diameter of the spool
d_spool_1 = 0.010; %m
%Area gradient = pi*d_spool
w_1 = pi*d_spool_1; %m
%Discharge coefficient
C_d_1 = 1;
%Valve natural frequency
omega_n_1 = 2*pi*50; %rad/s
%Valve damping ratio
xi_1 = 0.8;
%Supply pressure
P_s = 150; %bar
P_s = P_s * 1e+5; %Pa
%Tank pressure
P_t = 0; %bar
P_t = P_t * 1e+5; %Pa

%------------------------------------------------------------------------%
%------------- Spool valve parameters- Second cylinder ------------------%
%------------------------------------------------------------------------%
%Diameter of the spool
d_spool_2 = 0.010; %m
%Area gradient = pi*d_spool
w_2 = pi*d_spool_2; %m
%Discharge coefficient
C_d_2 = 1;
```

```
%Valve natural frequency
omega_n_2 = 2*pi*50; %rad/s
%Valve damping ratio
xi_2 = 0.8;
%Supply pressure
P_s = 150; %bar
P_s = P_s * 1e+5; %Pa
%Tank pressure
P_t = 0; %bar
P_t = P_t * 1e+5; %Pa
```

APPENDIX B. AMESIM BLOCKS USED

	Hydraulic items
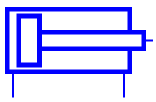	Double hydraulic chamber single rod jack supplying a force: includes pressure dynamics, viscous friction, and leakage.
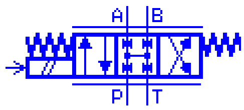	3 position 4 port hydraulic valve: Spool dynamics is modeled as a 2^{nd} order system.
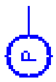	Piecewise linear hydraulic pressure source.
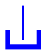	Tank modeled as constant pressure source.
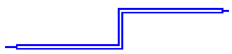	Compressibility + friction hydraulic line: These parameters of the hose are calculated using an effective bulk modulus.
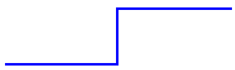	Hydraulic direct connection.
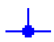	3-port hydraulic junction: The bold line indicates from which port the pressure is imposed to the sub-model.

	Signal/Control items
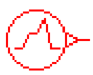	Piecewise linear signal source: It generates piecewise linear signals like ramps, steps, squares, saw tooth or trapezoidal signals.
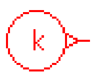	Constant signal: it generates a constant value.

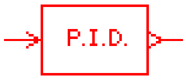	Proportional integral derivative controller (PID): Controller is defined by the gains Kd, Kp, Ki and Ks.
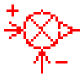	Comparison junction differencing inputs: The output signal at port 2 is the difference between the input signals at ports 1 and 3.
	Control direct connection.

Planar mechanical items	
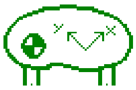	Rigid body accepting n-number of joints: The mathematical model is based on the Lagrange equations and it can be connected to any joint component.
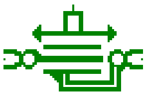	Translational actuator: The input from this port is a force that is sent to the planar mechanical ports.
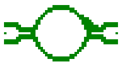	Revolute pair: The two constraint equations are obtained by expressing the coincidence of points at port 1 and 2.
	Reference fixed body: It can be considered as a zero acceleration, velocity and displacement source.
	Zero force source: It is a zero torque and force source.
	Planar mechanical direct connection

Mechanical items

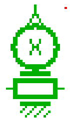	Displacement sensor with offset and gain: It is necessary to include a negative gain to get correctly the sign of the signal.
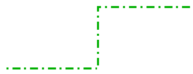	Mechanical direct connection

Cosimulation mode

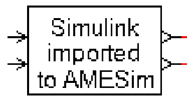	Simulink to Amesim block: transforms desired Cartesian coordinates to actuator displacement

Others

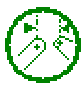	Generation of an assembly process before the simulation run.
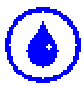	Indexed hydraulic fluid properties: It is used to set the characteristics of the hydraulic fluid.